6
Morphology and Properties of Spray-Dried Particles

Peter Walzel and Takeshi Furuta

6.1
Introduction

Spray drying is, by definition, the transformation of a feed of liquid (solution or dispersion) or paste material into a dried particulate powder. The feed liquid is atomized into small droplets of several dozens to a few hundreds μm, which are dried to the powder by contacting with a hot drying medium (Masters, 1991). The volume mean particle size of the powder is typically in the range $10\,\mu m < d_{V,50} < 1\,mm$, with mean particle sizes of $50\,\mu m < d_{V,50} < 300\,\mu m$ being more frequent in practice.

One advantage of spray drying over other drying methods is that the process leads directly and in a fairly simple way from a liquid feed to solid particles. Another crucial advantage is that drying is very rapid and can be completed in a very short time. Drying times between 5 and 30 s are typical for sprays with a droplet diameter of 10–200 μm according to Furuta *et al.* (1994). Furthermore, it is possible to form spherical powder particles by spray drying, and it is also possible to transport the product powder from the drying vessel to the storage bins pneumatically, that means by using the drying gas (typically air).

Spray drying plants commonly consist of a feed pump, an atomizer, an air heater, an air distributor, a drying chamber, and systems for exhaust air cleaning and powder recovery, as shown in Fig. 6.1. Atomization is the key technology in spray drying, because it determines the droplet size distribution, which – in its turn – has a great influence on both the size of the final powder and the kinetics of the process. Atomization is commonly performed by means of spray nozzles or centrifugal disk atomizers. The centrifugal rotary disk atomizer is favorably applied to highly viscous liquids and slurry feeds. It has the advantage of enabling easy control of the droplet diameter by varying the rotational speed of the disk. Spray nozzles may operate with one fluid (the pressurized liquid feed) or two fluids (the liquid feed and air). Two-fluid nozzles are an alternative for the atomization of highly viscous fluids, and a very good candidate when aiming at the production of very small (even submicron) particles. An overview of recent developments is given, for example, in Walzel (2001). Very small particles can also be produced by means of ultrasonic atomizers. In any case,

Modern Drying Technology Volume 3: Product Quality and Formulation, First Edition.
Edited by Evangelos Tsotsas and Arun S. Mujumdar.

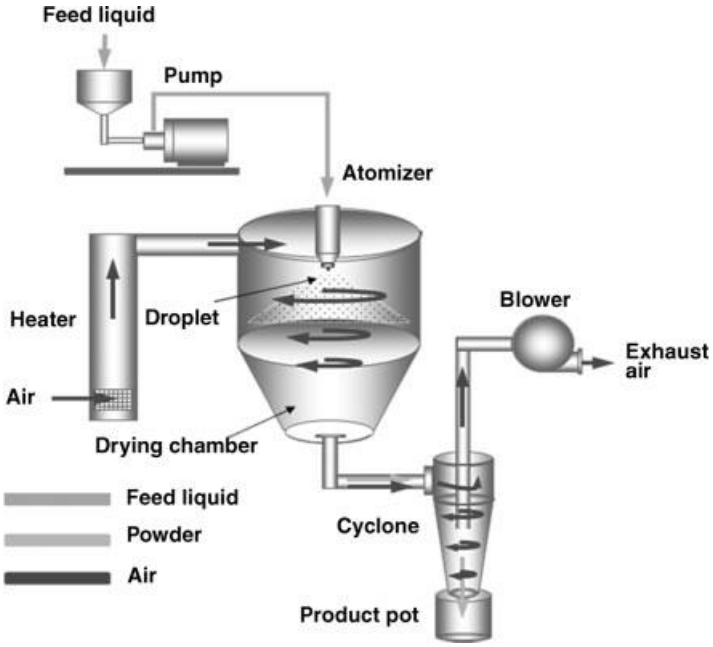

Fig. 6.1 Typical spray-drying system consisting of a feed pump, an atomizer, an air heater, an air dispenser, a drying chamber, and equipment for exhaust air cleaning and powder recovery.

atomization of the liquid feed to more or less fine droplets is the main reason for the mentioned fast kinetics of spray drying, due to a dramatic increase in surface area; (transformation of one large drop of 1 cm in diameter to many droplets of 100 μm increases the surface area by a factor of 100, and transformation to fine droplets of 1 μm increases it by a factor of 10 000).

The spray drying process is frequently operated concurrently regarding the gas and the spray flow, as depicted in Fig. 6.1. Under these conditions the thermal stress on the particles is low and even sensitive materials such as food, pharmaceuticals, cosmetics and other high value products can be dried. In other cases the thermal stress may be of little relevance, for example, when drying thermally resistant detergents or ceramics. Then, a partly countercurrent flow arrangement or a fountain-like spray pattern or even completely countercurrent arrangements can also be applied. Countercurrent flow between the gas and the droplets usually leads to significant particle collisions and agglomeration, and thus to larger particles.

During the spray drying process, the solution droplet may shrink due to the evaporation of solvent, which is most often water. By decreasing the water content and water activity, spray drying is generally used in the food industry to ensure the microbiological stability of products, avoid the risk of chemical and/or biological degradations, reduce the storage and transport costs, and, finally, obtain a product with specific properties such as instantaneous solubility. Typical spray-dried food products are listed in Tab. 6.1. It should be mentioned that over 80% of the

Tab. 6.1 Typical spray-dried food products.

Type of material	Ingredients
Flavoring agents	Oil, spices, seasonings, sweeteners
Vitamins	Vitamin E, β-carotene, ascorbic acids
Minerals	Calcium, magnesium and phosphorus
Oils and fats	Fish oils (DHA, EPA), sea buckthorn oil, lycopene
Herbs and bioactives	Creatine, probiotic bacteria
Other	Enzymes, leavening agents, psyllium, yeast

manufacture of food flavor powders involves spray drying. When the water content of the droplet reaches a critical value, a dry crust is frequently formed at the droplet surface. The morphology of the particles depends on the inlet and outlet air temperature. Commonly, if the droplet is dried very slowly, it is transformed into a fully dried particle. At high drying temperature, however, cycles of repeated expansion and collapse of the particle occur, due to the formation of an internal air bubble.

The internal and surface morphologies of spray-dried powders affect the powder flowability, re-dispersability, density, and the stability of the encapsulated active ingredients. The vacuole and surface roughness of spray-dried powders are important morphological characteristics with an influence on powder flowability. The quality factors of the particles are a direct result of the design and operating conditions of the spray dryer, such as the type of atomizer, drying air temperature, feed rate, and viscosity or nature of the solid matrix. The dissolved or dispersed solid concentration and the additives in the feed liquid, such as sugar, lipids, polymers, and proteins, also affect the morphology (i.e., size and degree of hollowness) of spray-dried powders (Hadinoto *et al.*, 2007).

The drying process of liquid droplets containing solid matter generates very different shapes and structures of the finally dried solid particles, as already described in Masters (1991). It is obvious that the structure of the solids depends on both the solid material, and the operational parameters such as air and liquid temperature and droplet size. Singe droplets in a large air volume may dry at a different rate compared to droplets incorporated within a dense spray, even at the same ambient air temperature. This is due to the decrease in the driving forces when many particles a short distance apart release their vapor and thus reduce the overall driving force. If this is the case, the shape of the spray jet may also influence the drying process, even at the same air inlet temperature (see Chapter 5 in Volume 1 of this series). The outlet gas temperature and outlet air humidity are also good indicators for the driving potential of the total drying process as well as the inlet air temperature. Furthermore, the product is usually discharged with a temperature fairly close to the outlet air or gas temperature. Only in the case of countercurrent operations do significant differences appear between air outlet temperature and the discharge temperature of the product.

Chapter 5 of Volume 1 described in detail how the flow patterns of hot air and the trajectories of the drying droplets can be analyzed by computational fluid dynamics

(CFD) to improve and optimize the drying system. In the present chapter, the morphology of spray-dried particles is examined as a function of the outlet air temperature and additives, such as surfactants and proteins. Scanning electron microscopy (SEM) and confocal laser scanning microscopy (CLSM) are used for the investigation of the outside and inside morphology of the spray-dried particles.

6.2 Morphology of Spray-Dried Particles

6.2.1 Classification of the Morphology of Spray-Dried Powders

Extensive studies of the particle morphology during drying have been performed by Walton and Mumford (1999a, b) and Walton (2000) by means of a single suspended droplet drying method. They classified the typical particle formation processes of a droplet containing dissolved solids, as illustrated schematically in Fig. 6.2. In the early stages of drying, the droplet has a free liquid surface, where

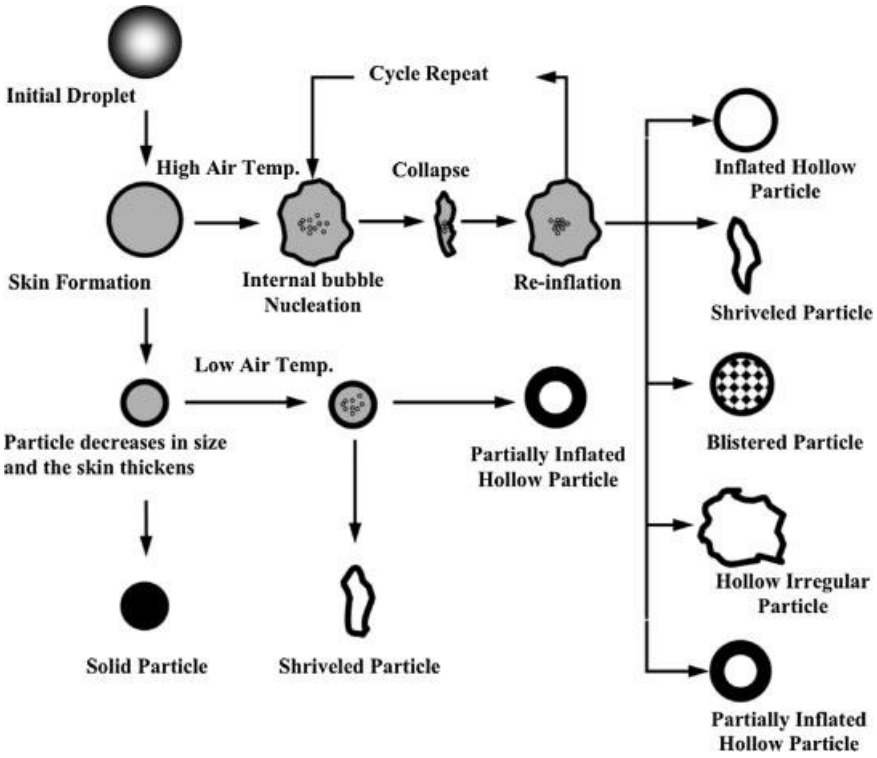

Fig. 6.2 Scheme for the particle morphology of skin-forming materials (modified from Walton (2000)).

water evaporates rapidly. The depletion of water content at the surface will cause the solute to be more concentrated – this will depend on the speed of evaporation and the rate at which the water can be replenished from the interior of the droplet. Because of the increase in concentration, solids may precipitate out of the solution at the surface of the droplet first, leading to the formation of a crust or skin around a hollow particle. The thickness of the crust will depend on the drying rate – high initial drying rates will lead to larger particles with thin shells and low density, whereas low initial drying rates will lead to smaller particles with thick shells and high density.

Another possible reason for the formation of hollow, high-porosity particles is the presence of occluded or absorbed gases in the feed liquid, which may lead to bubble formation, even below the boiling point. Once the particle has formed, it may remain intact or may fracture due to internal pressure. If the skin is pliable, then, depending on the drying conditions, it may puff up or collapse and shrivel. In the case of low air temperature, drying is slower during the surface evaporation period, so that the particle decreases in size and forms a thicker skin. In the falling rate period, bubbles may appear by nucleation due to temperature increase. Subsequent expansion and collapse of bubbles result in hollow particles or shriveled particles. However, if the nucleation is suppressed, the droplet will be dried to a dense solid particle. On the other hand, if the process takes place at high ambient or air temperature, repeated cycles of expansion and collapse of internal bubbles may occur after the skin formation, resulting in the various types of particles shown in Figs. 6.6 and 6.11 to 6.16. Mechanisms of bubble formation and expansion were discussed by Greenwald (1980) who concludes that a two step mechanism is operative:

- First, an air bubble is created by desorption of air which is either present in the feed liquid or absorbs shortly below the atomizer (Greenwald and King, 1981, 1982). Alternatively, such an air bubble may be incorporated during atomization (Verhey, 1972a, b, 1973).
- The second step needed to bring about expansion is that of the drop temperature approaching or exceeding the boiling point, whereupon a large amount of water vapor will be formed in the bubble, causing it to grow substantially in size.

The largest effect on particle morphology is, however, given by the composition and solid materials contained in the liquid to be sprayed (Walton, 2000; Jørgensen, 2005). Several different options exist concerning the composition of the slurry:

- solution of low molecular weight substances (crystallization and crusts)
- solution of high molecular weight substances such as polymers (skin forming)
- suspension of (insoluble) small solid particles, $d < 2\,\mu m$ (crust forming)
- suspension containing large solid particles $d > 5\,\mu m$
- complex dispersions such as, for example, emulsions and other formulations.

The formation of different morphologies can either be studied in large scale spray dryers or in specially designed spray dryer pilot plants, see for example Zbicinski

et al. (2002a, b), Jørgensen (2005). A further option is to observe the drying process within a levitator (Toei *et al.*, 1978; Kastner *et al.*, 2001; Brenn *et al.*, 2001; Groenewold *et al.*, 2002). This device allows the suspending of particles at a stable position within the gas environment. These particles have a size of typically $d > 300\,\mu m$ and can be dried on a lab scale under distinct and defined conditions. Another option is the drying of droplets suspended on a wire which also gives some insight into the structure-forming process (Hecht and King, 2000a; Dicoi and Walzel, 1998).

The particle size, d, can be calculated from the diameter of the spray droplets, d_d, and the solid mass fraction of the solution or suspension, x_s, according to the relationship

$$d = d_d \left\{ (1-\varepsilon) \left(\frac{1-x_s}{x_s} \frac{\varrho_s}{\varrho_l} + 1 \right) \right\}^{-1/3} \tag{6.1}$$

Here, ϱ_s is the solid density and ϱ_l the liquid density. Due to the small magnitude of the exponent, only strong variations in concentration, densities and porosity lead to significant differences between particle size and droplet size. However, the overall porosity, ε, of the final spray-borne particle may indeed be strongly affected by the formation of solid structures during the drying process. It is not known in advance and so far can only be determined experimentally, which also holds for particle density. Particle porosity lies in the relatively narrow range of $0.5 < \varepsilon < 0.6$ only for relatively large and rather compact particles that exhibit approximately uniform distribution of voids throughout their whole cross-section.

Typical examples of particle structures as formed by the drying process and depending on the solid matter contained in the liquid feed will be given in the following.

6.2.2
Solutions of Low Molecular Weight Substances

When spraying solutions of substances of low molecular weight, a first drying step occurs above the solubility limit of the solute, and the drop reduces in size until the solubility limit is reached. For this first step, which is usually called the first or constant rate period (CRP), the drying velocity, that is, the solvent mass evaporated per unit time, is given by the vapor pressure of the solution at the drop surface, $p_{v,S}$, and the vapor pressure in the vicinity of the particle, $p_{v,\infty}$. The vapor pressure at the surface depends – assuming a well-mixed state within the droplet – on the drop temperature and on the water activity within the solution. The surface temperature remains low in the CRP as the solvent, due to its heat of evaporation Δh_v, uses up the sensible heat (expressed by the specific heat capacity $c_{P,v}$ of the air–vapor mixture) transferred to the particle by the gas in a hot atmosphere. The particle surface temperature T_S is more or less close to the wet bulb temperature of pure water, depending on the water activity in the case of dissolved matter (see Eq. 5.44 in Volume 1 of this series). The dependence of the vapor pressure of the solvent on the surface temperature T_S may be expressed by the Antoine or Clausius–Clapeyron equation, as

in Volume 1 of this series, Eq. 5.36. The surface temperature T_S is also linked to the mass transfer coefficient k, the heat transfer coefficient α, the total gas pressure P, and the gas temperature T_∞ at a sufficiently large distance from the surface according to the relationship

$$\alpha \frac{\Delta h_v}{c_{P,v}} \ln\left[1 + \frac{c_{P,v}}{\Delta h_v}(T_\infty - T_S)\right] = k \frac{\Delta h_v \tilde{M}_v P}{\tilde{R} T_m} \ln \frac{P - p_{v,\infty}}{P - p_{v,S}} \tag{6.2}$$

(see Bird *et al.* (2002), Jørgensen (2005), Gnielinski *et al.* (1993), Abramzon and Sirignano (1989), and Volume 1 of this series). Here, T_m is the mean temperature between the particle and the air. As soon as the solubility limit is reached at the drop temperature, crystallization of the solute may set in. Supersaturation is due to evaporation, and, therefore, highest close to the surface of the droplet, where the evaporation takes place. Hence, crystallization will start from there. Depending on the nucleation properties of the solute, more or less nuclei are formed at the surface until a solid layer of crystals builds a crust. Depending on the permeability of the crust, solution can be transported through small capillaries between the crystals whereas the surrounding gas can enter through large capillaries to compensate the low internal pressure. As a result, hollow beads are formed consisting of a poly-crystalline shell. Some basic considerations help us to understand the behavior of solid phase formation and the morphology of particles.

High solute and air temperature usually mean higher solubility and higher mass content before the onset of crystallization. (However, some materials do not show increased solubility with increased temperature, as e.g., NaCl). High solubility also means a late onset of crystallization and low solvent content. Due to this fact, particles should form a shell with a thick wall. Materials with low solubility, but still sprayed into the dryer as a solution, are expected to form a thinner shell. However, the nucleation properties, such as nucleation rates and the growth rates of crystals, also play a major role. Some materials do not form crystals but solidify in an amorphous or glassy state. A typical example is lactose, for example, sprayed as a 20 wt% solution into air at an air exit temperature of 90 °C, as shown in Fig. 6.3.

Some materials exhibit a rubbery state in the case of too high temperatures or water content. Such materials are difficult to dry due to their sticky surface. For this reason it is necessary to know the glass transition temperature, T_g, below which the surface becomes hard enough to avoid lumping. The glass transition also depends strongly on the water content (Gordon and Taylor, 1952). A typical example is maltodextrine, see, for example, Bröckel *et al.* (2007). Single drop measurements of drying kinetics and stickiness have been presented for different hydrocarbon solutions by Adhikari *et al.* (2003). Acid-rich foods such as fruits, juices and vegetable juices, and sugar-rich components belong to the group of sticky products with low T_g. These materials are very difficult to dry in normal spray drying equipment due to the requirement of low temperature and the high residence time resulting from the low driving force. In foods, starch, such as maltodextrine, is very often added as an anti-sticking agent and drying aid; (for the glass transition temperature of maltodextrine see also Kilburn *et al.* (2005)). Freeze spray drying, which will be briefly discussed in Section 6.2.7, is

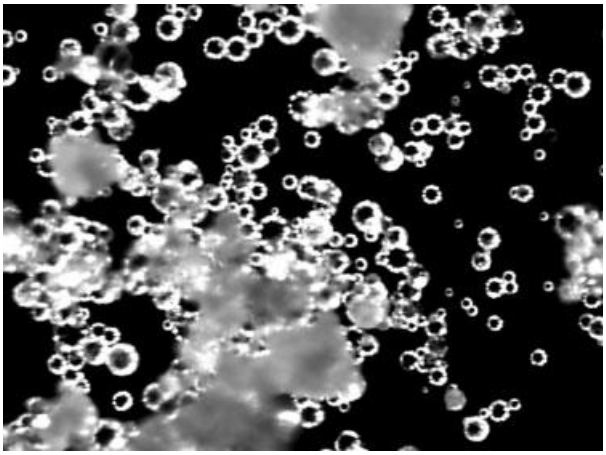

Fig. 6.3 Glassy lactose particles obtained from a 20 wt% aqueous solution at an outlet air temperature of 90 °C; Mean particle size: $d = 65\,\mu m$. The transparency of the particles is a clear indicator for the absence of larger crystals.

an option when no additives are allowed to modify the surface properties of the particles. However, freeze spray drying is more costly.

When comparing small and large drops under the same driving force conditions, the drying of smaller drops is faster due to the higher mass and heat transfer. This affects the nucleation and growth of crystals, as the supersaturation increases with decreasing drop size. There are several competing timescales, the most important being those for mass transfer, nucleation and the growth rate of the crystals. Nucleation and growth rate are different for different materials (Gnielinski *et al.*, 1993). This is one reason for the different morphologies of small and large particles. Another reason is the different trajectories of large and small particles within the dryer. Small particles may recirculate in a hot air stream while large particles escape more easily from turbulent eddies and follow the influence of gravity to a much larger extent.

In Brenn *et al.* (2001) a proposal is presented for distinguishing between the formation of hollow beads and compact particles obtained from crystallizing substances by means of the parameter

$$G = \frac{D_l \varrho_l}{D_g \varrho_g} \frac{1}{Sh^* \ln(1 + B_M)} \tag{6.3}$$

The model was validated on NaCl solutions. In Eq. 6.3, D_l is the diffusion coefficient of the solute in the liquid phase, D_g is the diffusion coefficient of the solvent vapor in the gas phase, ϱ_l and ϱ_g are the liquid and gas densities, respectively. Sh^* is the dimensionless mass transfer rate in the vapor phase. This modified Sherwood number, that accounts for the film thinning effect of Stefan flow, lies typically in the range $2 < Sh^* < 5$. The quantity B_M is the Spalding transfer number according to Abramzon and Sirignano (1989) (Sirignano (1999), compare with Eq. 1.66 in Volume

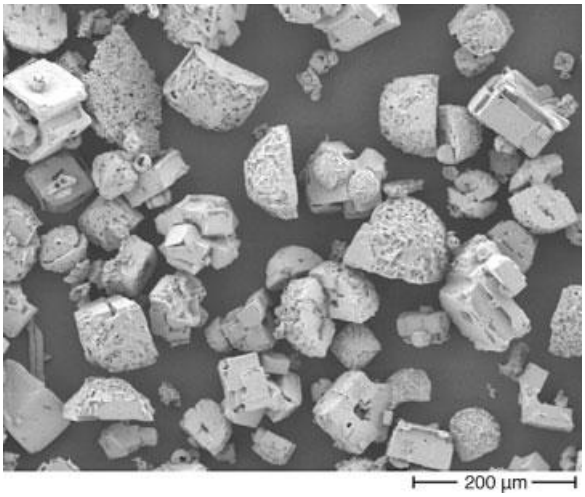

Fig. 6.4 Example of a simple crystallizing material (NaCl particles after spray drying from 20 wt% solution). No significant difference in the particle shape was found at air inlet temperatures of 140 up to 220 °C. Cubic and hemispherical-shaped particles are visible. Some particles show a void space in their center.

2 of this series). When $G > 3.3$ solid particles are formed, whereas hollow particles are expected for $G < 3.3$. The latter takes place when the gas-side mass transfer rate is high and when the diffusion rate of the solvent in the droplet is comparatively small. Figure 6.4 shows particles formed from 25 wt% NaCl solution in water. Only a few particles exhibit hollow structures as G was in the range $5 < G < 6$.

Many materials such as salts, for example, Na_2SO_4, show different stable modifications for given temperatures with different content of crystal water. Usually, a stable modification is formed first, at the given drop or particle temperature. The hygroscopic property of the product may then be the result of a subsequent transformation into a different modification stable at ambient temperature and humidity. As the lattice of the crystals is restructured during uptake of water from the ambient air, the strength of the particle may diminish and dust can be formed.

The surface structure of spray-dried particles can be regarded as a key for fine particle adhesion in customer applications. This effect is needed for example, for inhalation therapies when fine active particles with $d < 5$ µm are added to spray-dried carrier particles within the size range 60–100 µm in order to obtain a dose unit with reasonable flowability and with proper detachment properties of the fines. Experiments with mannitol (Maas *et al.*, 2009) gave rise to quite different surface morphologies when sprayed into air at different temperatures. In the case of low air exhaust temperatures, $T = 80$ °C, the carrier particles exhibit a fairly smooth surface. At an exhaust air temperature of $T = 130$ °C, the particles show rough surfaces formed by crystals covering the particle surface, see Fig. 6.5. In this case, the air temperature is a vehicle to adjust the desired adhesion properties.

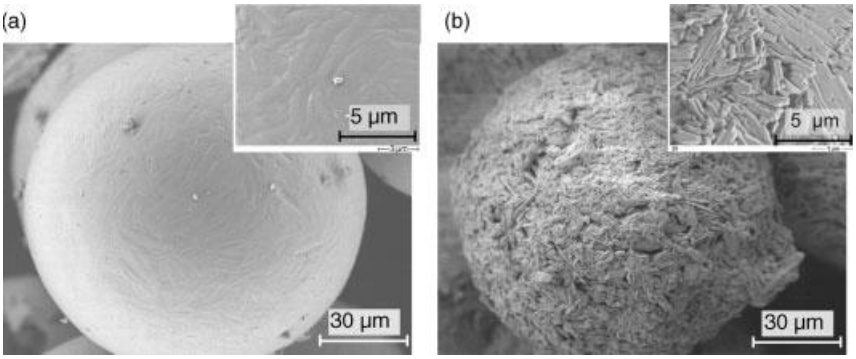

Fig. 6.5 SEM of mannitol particles obtained from 15 wt% solution at a dryer exhaust temperature of (a) 80 °C and (b) 130 °C.

6.2.3
Solutions of Polymers

When spraying solutions of polymers, the spraying process is usually limited to viscosities less than 0.5 Pa s under spraying conditions. Higher viscosities give rise to the formation of fiber-particle mixtures and deformed spheres. Finally, at $\mu > 10$ Pa s only fibers are formed (Lohner *et al.*, 2005; Eggers and Villermaux, 2008). The same behavior can be observed when highly viscous melts are sprayed, see for example, Walz and Mayer (1966).

The vapor pressure of the solvents in the presence of large solute molecules is reduced during the drying process. The solvent activity can then be described by the Flory–Huggins equation (Flory, 1942; Shinoda, 1978; Vrentas and Vrentas, 1996). Besides phase equilibria, the diffusion of the solvent is usually significantly reduced, decreasing strongly with increasing solids content, especially close to the particle surface. The reduced penetration of the solvent through the resulting shell leads to significantly reduced evaporation, and to a considerable rise in the particle temperature. While a thin skin-like shell is formed on the surface, the inner part of the droplet remains in a liquid state. As the cooling effect of the evaporating solvent ceases, the droplet reaches the air temperature, mostly higher than the boiling point of the solvent. Bubbles appear in the droplet and the vapor finally penetrates the shell, forming a blowhole. As a result, particles show indentations and sometimes an irregular structure. This process may be repeated several times, so that the shape of the particles becomes more and more irregular, as shown in Figs. 6.6 and 6.7 with styrene–butadiene–styrene (SBS) latex.

6.2.4
Suspensions Containing Small Solid Particles

In the case of small insoluble primary particles with a diameter of, typically, $d_{v,50} < 2\,\mu$m within the droplet, the drying process takes place from the outer shell,

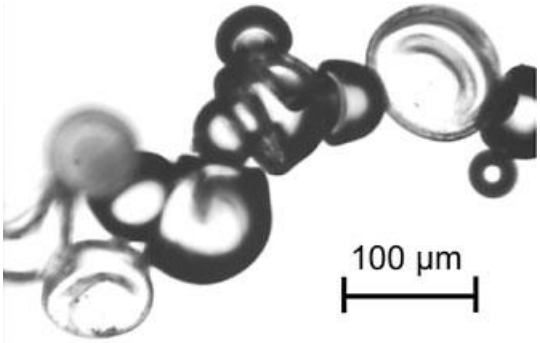

Fig. 6.6 SBS-latex particles dried at moderate air inlet temperatures, such as 120 °C. The particles are hollow and show indentations due to collapse of the skin.

reducing steadily the size of the drop. Such conditions appear when spraying suspensions. A typical application is the preparation of ceramics. In the production of ceramics, spray drying is usually followed by a further compaction of the bulk material by external pressure and, finally, by a sintering process (Nebelung *et al.*, 2008).

At a high speed of shrinkage, the diffusion rate of solids accumulated with a high concentration in the outer regions of the suspension droplet is not fast enough to equalize the particle concentration difference within the drop. The diffusion coefficient D_{sp} of suspension particles with diameter d_p is usually about 1 to 4 orders of magnitude smaller than, for example, low molecular solutes. It can be estimated from the relationship

$$D_{sp} = kT/(3\pi\mu d_p) \tag{6.4}$$

where k is the Boltzmann constant, T the temperature in K and μ is the viscosity of the dispersing agent. A bridge or shell-like structure is formed by the primary particles

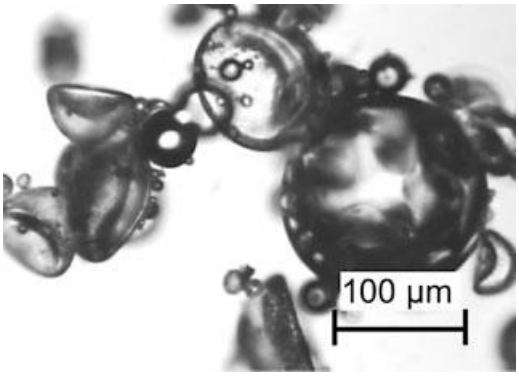

Fig. 6.7 SBS-latex particles dried at higher air temperatures, such as 160 °C. The particles are hollow and have bubbles in their interior as well as indentations due to collapse of the skin.

when they come into contact. As there are only fairly small pores between small particles, the "filtration" resistance of the particle system is high and the resulting outward liquid flow is small. Whereas liquid flows mainly through the small pores, air penetrates in the reverse, inward direction through larger pores (Koch and Walzel, 2001). Due to the capillary effect, this leads to a considerable under-pressure within the particles, causing the shell to bend inwards forming indentations or dimples or even a donut-like shape.

For suspensions, Minoshima *et al.* (2001, 2002) proposed a model based on the buckling behavior of the crust. According to this model, a particle is allowed to shrink as long as the buckling pressure is larger than the permeation pressure of the evaporating fluid. The buckling pressure depends on the shell thickness as

$$P_B = \{1/[2(d_d/d_{shell})-1]\}^2\{8E/[3(1-\nu^2)]^{1/2}\} \quad (6.5)$$

Here, E is the Young's modulus of the primary particles, ν is the Poisson number of the material, d_d is the drop diameter and d_{shell} is the inner shell diameter.

The mobility and softness of the shell consisting of primary particles also depends to a large extent on their electrostatic charge or ζ-potential. High ζ-potentials mean high charges of equal sign on the particles and repellent forces, whereas low or zero ζ-potential leads to immediate agglomeration and fixation of the position at which particles first come into contact. Therefore, structures with large pore volumes appear in the case of low ζ-potentials and structures of higher density arise when the particles can move, even when in contact with neighboring particles, and find a more stable position within the bulk. Highly stabilized suspensions, that is, those with high ζ-potentials, have a low viscosity and are easier to spray; they give rise to hollow particles with a fairly dense shell, quite similar to the case of crystallizing solutes. An example of these structures formed from 0.8 μm Si_3N_4 primary particles is given in Fig. 6.8. The stabilization usually is obtained by a pH-shift or by dispersants (polyelectrolytes). In the case of suspensions with low stability, no large central cavities are formed within the particles, so that particles of low but uniform density are formed. This particle structure is desired if a high density is to be achieved by subsequent pressing of the powder.

Flash spray drying of suspensions was examined by Monse *et al.* (2001). Suspensions of $BaSO_4$ particles with a primary particle size of $d_{V,50} = 1.7$ μm were sprayed. The suspension was heated to temperatures within the range $140\,^\circ C < T < 160\,^\circ C$ and flashed through a swirl nozzle into the tower with an outlet air temperature of about 160 °C. Figure 6.9 shows the morphology of the particles obtained from superheated and flashed (Fig. 6.8b), as well as from non-flashed (60 °C, Fig. 6.8a) suspensions.

The particles generated during the flash process have much higher density and only a small cavity in the center. This effect can be explained by the sudden immobilization of the primary particles throughout the agglomerate when a considerable part of the suspending liquid suddenly evaporates. In contrast, the non-superheated spray operation at the same drying air temperature gives rise to donuts

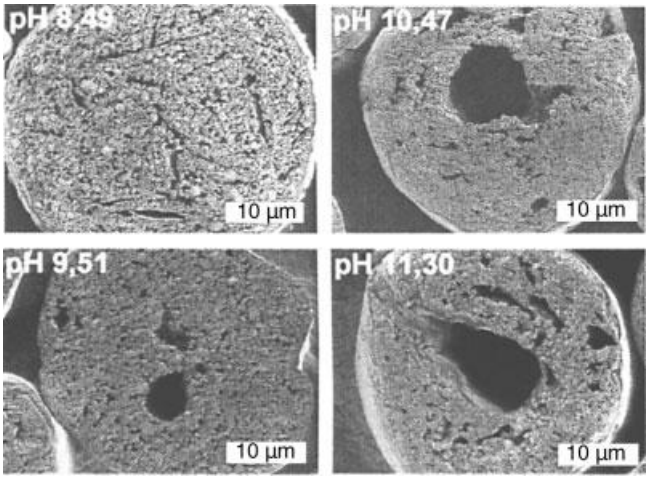

Fig. 6.8 SEM pictures of spray-dried particles generated from Si_3N_4-suspensions with different degrees of stabilization (Fries, 2008).

and to particle shapes with a large central cavity. The stabilization state of the suspension was reasonable in all cases with $\zeta = +40$ mV at a pH of 7.2. CMC (CRT 2000 GA from Wolff Cellulosics) was added as a binder (0.2% by weight related to the mass of $BaSO_4$). The $BaSO_4$ mass fraction of the slurry was 60%.

Smaller primary particles lead to a higher strength of the agglomerate spray particle (Rumpf, 1975). However, the strength may still be insufficient for the subsequent treatment of the product. It is, therefore, often necessary to add some binder, which helps to provide the necessary adhesion between the primary particles, even in the dry state. Different binders are known such as carbon hydrates

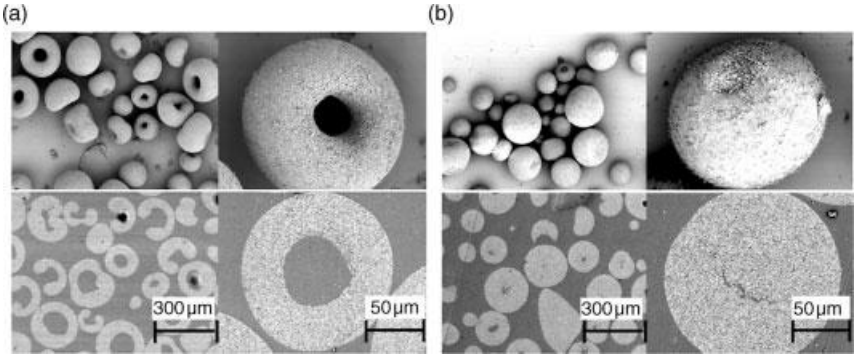

Fig. 6.9 SEM photos of spray-dried $BaSO_4$-suspension particles: Upper part of figure shows the outer appearance, lower part of the figure shows the cut through particles. (a) Donut-like particles produced at a suspension feed temperature of 60 °C; (b) particles obtained from superheated suspension at a feed temperature of 160 °C. The particles are less porous and show only small holes or cracks in the particle center. (Monce *et al.*, 2001).

(for example CMC), sugar, starches, molasses, gelatin, alginates, carrageenes or polyvinylalcohol, polyvinylpyrrolidone, polyacrylates and polyethyleneglycol, as well as silicon dioxide in different precipitation states. The addition of binder often further lowers the permeability of the crust and gives rise to stronger indentations and to the formation of hollow particles or donut-shaped particles (Jørgensen, 2005). For an investigation of the spray drying of TiO_2-, SiO_2- and Al_2O_3-slurries with different kinds of additives see also Jørgensen (2005).

In general, high drying temperatures ($T > 150\,^{\circ}C$) and small primary particles of the slurry ($d < 5\,\mu m$) give rise to the formation of hollow particles or particles with indentations; low temperature drying conditions ($T < 150\,^{\circ}C$) lead to uniform and compact particles. Highly concentrated slurries also lead to compact particles, as there is no space for the primary particles to rearrange their configuration during the drying step.

6.2.5
Suspensions Containing Large Solid Particles

Large primary suspension particles, that is, usually particles with $d_{V,50} > 5\,\mu m$, provide a higher permeability of the pore system emerging during spray drying. Consequently, the liquid is transported through the pores outwards much more easily than in the small primary particle system and the shell remains wet for a longer time. The larger pores also lead to a smaller capillary, that is, indentation pressure. Due to that fact, drops from these suspensions have been observed to dry most likely into a compact non-hollow particle (Jørgensen, 2005). However, in this case binders are mandatory to avoid fracturing of the agglomerated spray particles even with cautious handling. Furthermore, the viscosities of suspensions consisting of coarse particles are lower, so that such suspensions can usually be sprayed with higher solids content, which again contributes to a more uniform distribution of the voids within the particle.

6.2.6
Complex Dispersions Such as Emulsions and Other Formulations

6.2.6.1 Hard Shell Particles

Sometimes particles with a hard but permeable shell are desired. This is, for example, the case for catalyst particles in FCC processes like VPO precursors (Contractor *et al.*, 1987). These agglomerated particles containing the active catalyst are used within a circulating fluidized bed to perform redox reactions at high temperatures. Hard thermal-resistant and abrasion-resistant shells can be obtained by adding precipitated silicon oxide to the precursor suspension before spray drying (Uihlein, 1993; Koch and Walzel, 2001). During the drying process, the nanosized silicon oxide colloids migrate, together with the suspending liquid (water), through the small pores towards the surface of the spray particles forming a gel and glueing the primary particles there. In compensation, air penetrates inwards through the large pores to equalize the negative pressure. The large pores are then emptied from

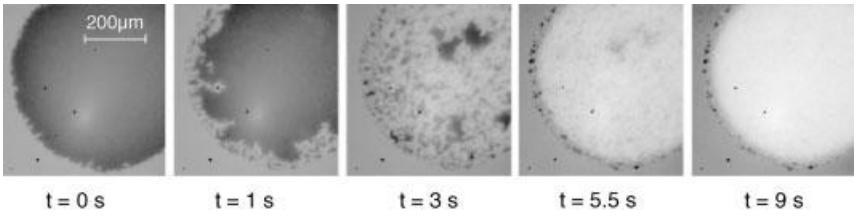

Fig. 6.10 Drying of a hemispherical suspension particle on a cooled glass sheet. Left to right: Intrusion of air fingers, formation of wet isles, migration of colored (dark) liquid towards the surface and deposition of the dissolved dark color at the outer rim of the particle.

the liquid. These pores later provide the necessary access for the gas to reach the active sites of the catalyst and the silicon oxide shell persists even during the tempering of the catalyst.

Experiments with suspension droplets deposited as half spheres on a cooled glass surface allow observation of the drying and migration process on a microscope from below when these droplets are subjected to a hot gas flow (Monse *et al.*, 2006). The initial drop in Fig. 6.10 consisted of a 40 wt% suspension with 4.5 µm $BaSO_4$ particles in water also containing 5% dissolved black color. First, the intrusion of air fingers into the large pores in the outer rim of the droplet can be observed. Later, there are some isles of liquid (dark) left within the internal part of the droplet. As the drying proceeds, liquid is transported through the small channels or pores between the beads towards the surface. Simultaneously, the dissolved color is carried along with the liquid and is finally deposited close to the surface, where it remains as a dried layer. The same occurs when a gel such as silicon oxide is dissolved in the liquid. However, the viscosity of the gel must be low enough for the migration process. The large pores stay open and allow gas penetration into the core of the particles, as this is required for catalysts.

6.2.6.2 **Gelatinization**

In the case of starch, one has to consider gelatinization effects taking place at high drying temperatures. This has a strong influence on the morphology. In Jørgensen (2005), experiments were carried out with maize and rice starch suspensions at different ambient air temperatures. At drying air temperatures of $T > 200\,^{\circ}C$ hollow particles were formed with high contents of gelatinized material in the case of rice starch. This is an indication that temperatures within the particle were beyond the gelatinization temperature of rice starch (70 °C). At air temperatures of $T < 150\,^{\circ}C$ the primary starch particles remain separate and non-hollow particles are formed with uniform and compact structures throughout the cross-sections. However, these particles have low mechanical strength.

6.2.6.3 **Microencapsulated Flavor Powders Formed from Emulsions**

In studies of the morphology of encapsulated flavor powders, scanning electron microscopy (SEM) has been commonly used to observe the porosity and surface integrity (Rosenberg *et al.*, 1985; Kim and Morr, 1996; Ré and Liu, 1996;

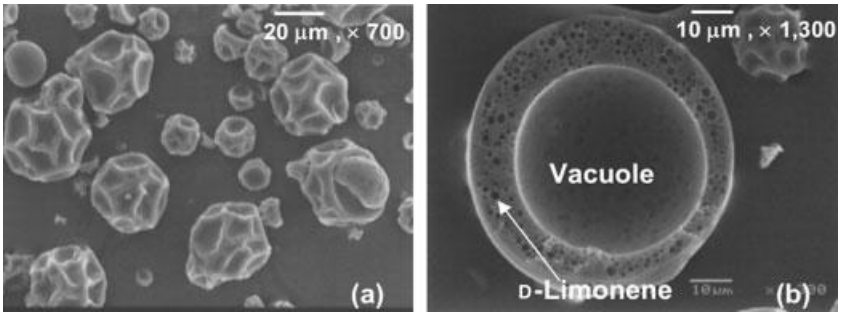

Fig. 6.11 SEM picture of (a) outside and (b) inside structure of spray-dried particles. The active core material (D-limonene emulsion) is in the form of small droplets embedded in the shell region of the carrier matrix (b). In the center of the capsules, a large void can be observed which occupies most of the capsule volume.

Soottitantawat *et al.*, 2003, 2004b, 2007). Several techniques have also been developed to provide information about the inner microstructure of the microcapsules (Moreau and Rosenberg, 1993). Figure 6.11 shows typical SEM pictures of the outside and inside structure of spray-dried particles (Soottitantawat *et al.*, 2003). The inner structure of spray-dried particles obtained from emulsions is expected to contain the active core material (here D-limonene emulsion) in the form of small droplets embedded in the shell region of the carrier matrix. In the center of the capsules, a large void can be observed which occupies most of the capsule volume. The formation of the central void can be related to the expansion of the capsule (Chang *et al.*, 1988; El-Sayed *et al.*, 1990; Maa *et al.*, 1997; Hecht and King, 2000a, b). These quality factors are a direct result of the design and operating conditions of spray drying, such as the type of atomizer, drying air temperature, feed rate and feed concentration, and the viscosity or nature of the carrier materials (El-Sayed *et al.*, 1990; Onwulata *et al.*, 1996; Finney *et al.*, 2002). Hollow particles are produced at higher air temperatures due to the expansion of air bubbles in the droplets during the drying (Verhey, 1972a, b, 1973; Greenwald and King, 1981; Alamilla-Beltrán *et al.*, 2005).

In order to observe the encapsulated flavor droplet (emulsion) inside the spray-dried particle, ethyl-*n*-butyrate was used as a model flavor. Nile Red was dissolved in the ethyl-*n*-butyrate and served as a fluorescein probe of the oil phase (ethyl-*n*-butyrate emulsion) of the solution. Flavor labeled in this way was added to the carrier solution and emulsified. Figure 6.12 presents the results of the application of CLSM to investigate the morphology and the arrangement of encapsulated flavor droplets in the spray-dried powder. The images shown in Fig. 6.12a were produced by merging three kinds of CLSM pictures made with an Argon laser (for sodium fluorescence in a green color), with a He–Ne laser (for Nile Red in a red color), and transmission pictures for a particle with (right-hand side) and without (left-hand side) a vacuole. Figure 6.12b depicts merged images from CLSM with the He–Ne laser and transmitted images, in order to more clearly observe the – labeled – droplets of flavor in the powder (Soottitantawat *et al.*, 2004b).

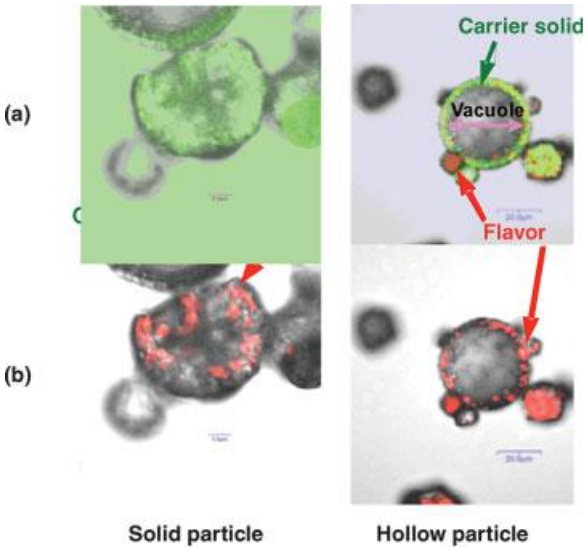

Fig. 6.12 CLSM pictures of the morphology and the arrangement of encapsulated flavor droplets in the spray-dried powder; merges of transmitted images with (a) CLSM images for sodium fluorescence in green color and for Nile Red in red color, (b) He–Ne laser CLSM images in red color (Soottitantawat *et al.*, 2004b). Droplets of flavor in the particles become visible especially in part (b) of the figure. Compact particles (left-hand side) can clearly be distinguished from particles with vacuole (right-hand side).

The photos of Fig. 6.12 visualize in a non-destructive manner the distribution of emulsion flavor droplets (red color) over the cross-section of the spray-dried powder and the internal morphology of the product (i.e., the presence, or not, of a vacuole). Therefore, they show that the CLSM is a new valuable tool for studying and observing the encapsulated flavor. The technique can even be applied to study the release characteristics of flavor from the powder in real time (Yoshii *et al.*, 2007).

6.2.6.4 **Particles from Proteins, Enzymes and Carrier Materials**

In the last decade confocal laser scanning microscopy (CLSM) was shown to be a helpful tool for various further tasks of microparticle characterization (Lamprecht *et al.*, 2000a, b, c). It minimizes the light scattered from out-of-focus structures, and permits the identification of several compounds through use of different fluorescence labels. Therefore, CLSM can be applied as a non-destructive visualization technique for microparticles. Moreover, CLSM allows visualization and characterization of structures not only on the surface, but also inside the particles, provided the carrier matrices are sufficiently transparent and can be fluorescently labeled; by collecting several coplanar cross-sections, a three-dimensional reconstruction of the inspected objects is possible. Figure 6.13 shows the application of CLSM to investigatation of the cross-sectional structures of spray-dried powders of maltodextrin (MD) with a dextrose equivalent value of DE = 2 and 20. Florescein sodium salt was dissolved in the feed solution as a fluorescent probe of the carrier

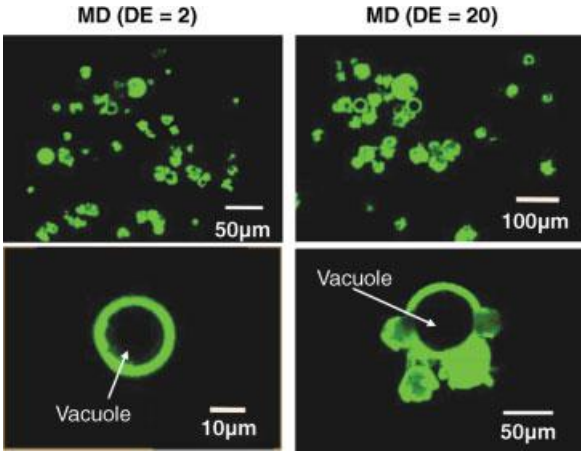

Fig. 6.13 The cross-sectional structures of spray-dried powders, observed by CLSM (MD, DE = 2 and 20). Florescein sodium salt was dissolved in the feed solution to mark the carrier solid. As only fluorescent material can be detected by CLSM, spray-dried particles containing a vacuole appear as green fluorescent rings.

solid. The laser supplied a 485 nm excitation wavelength allowing emission of the fluorescein sodium at excitation/emission wavelengths of 485/530 nm. Since only fluorescent material can be detected by CLSM, the shells of spray-dried particles containing vacuoles are observed in the form of green fluorescent rings (Soottitantawat *et al.*, 2007).

Figure 6.14 shows the SEM and CLSM pictures of spray-dried powder morphology for blends of GA-MD (GA: gum Arabic) as the carrier solid. Dextrose equivalent values of MD vary between 2 and 25; trehalose is also shown to represent the limiting case of a carrier material with a very high DE value (Soottitantawat, 2005). According to the SEM pictures of the surface structure of the powder, the powder shows a deeper surface grooving at low DE values. The grooving of the surface was observed to be less deep at higher DE values, so that the particles are smoother.

Particularly for trehalose, no vacuoles inside the particles could be observed. The volume ratios of the vacuole to the powder observed by using CLSM for 300 randomly selected particles are shown in Fig. 6.15 as a function of the DE value of the carrier material of the powder. The volume ratio is nearly constant till a DE value of 11, and then decreases sharply with increasing DE value, reaching zero for trehalose. The behavior of trehalose can be easily anticipated from the results of Fig. 6.14.

The outer surface morphology of spray-dried trehalose/alcohol dehydrogenase (ADH) powder, with the addition of different amounts of bovine serum albumin (BSA) or β-lacto-globulin (Lg) is illustrated in Fig. 6.16 (Yoshii *et al.*, 2008). The particle surface appears smooth in the case of ADH alone, no grooves could be found.

However, the addition of proteins (BSA or Lg) in the feed solution affects the appearance of the particles. Fine grooves appear when the mass ratios of β-Lg or BSA to ADH are higher than 0.5. The increase in protein content deforms the surface of

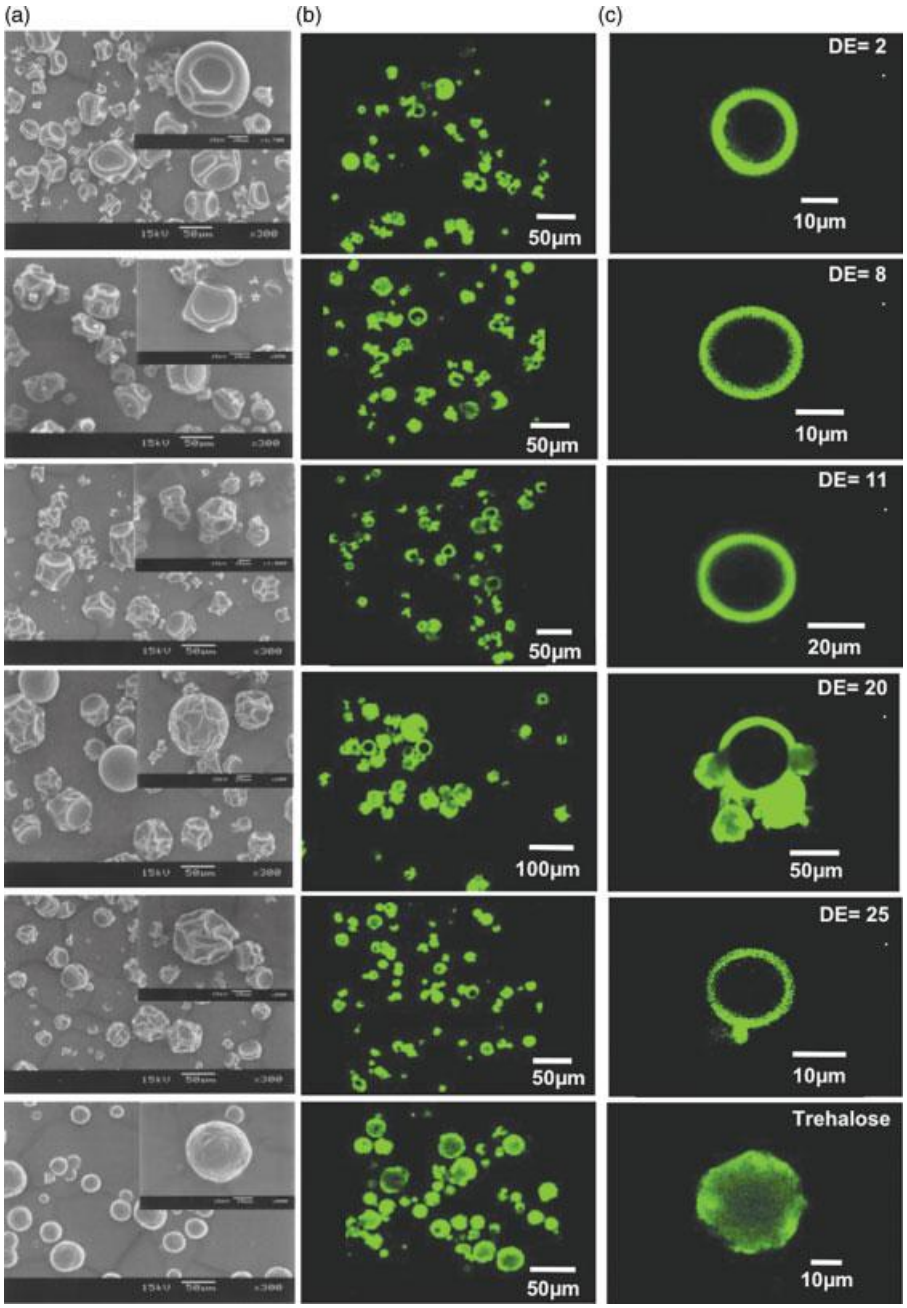

Fig. 6.14 (a) SEM and (b) and (c) CLSM pictures of spray-dried powder morphology for blends of GA-MD as the carrier solid. The dextrose equivalent value (DE) of MD was varied between 2 and 25; trehalose represents a very high DE value.

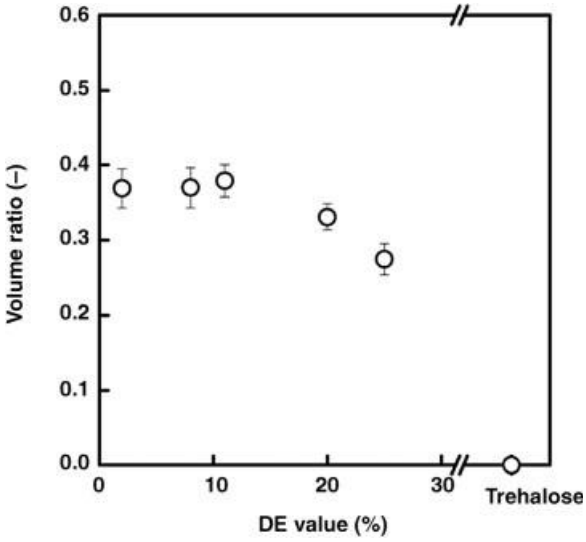

Fig. 6.15 Volume ratio of vacuole to total particle as a function of DE values of MD of the carrier material. Spray-drying conditions: Inlet air temperature 180 °C, atomizer rotational speed 30 000 rpm. The error bars show the standard error of the mean of 40 samples.

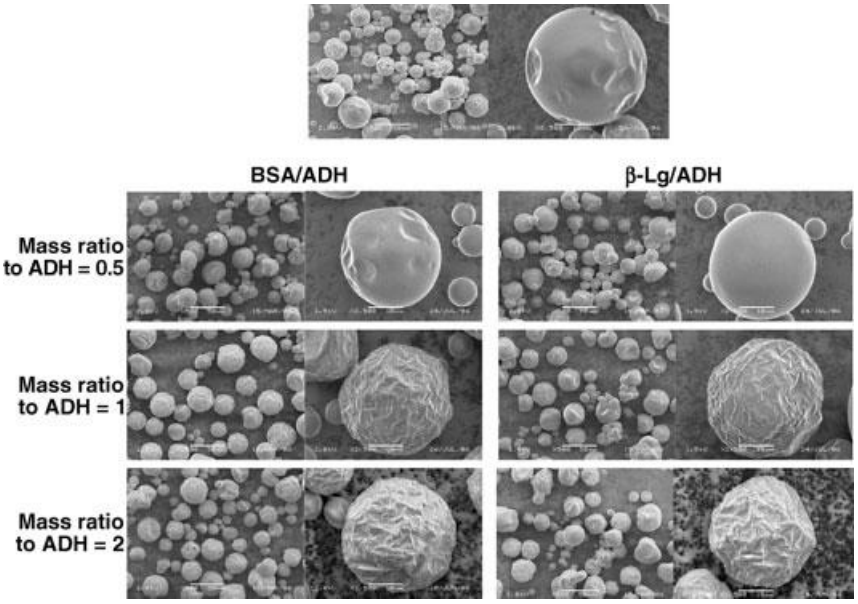

Fig. 6.16 Effect of addition of BSA and β-lactoglobulin on the spray-dried particle morphology; (trehalose mass fraction 30%, ADH content: 0.23 mg ADH/g trehalose, standard drying conditions).

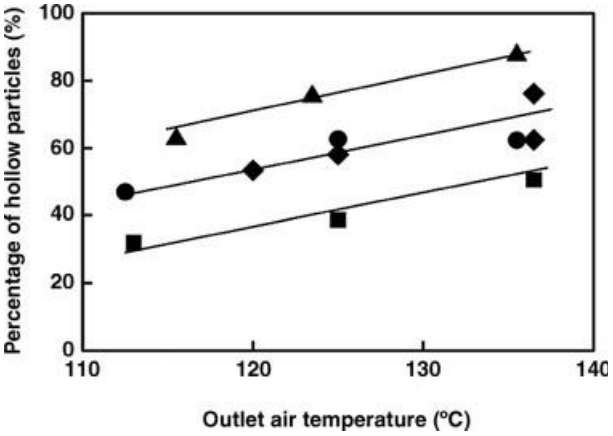

Fig. 6.17 The effect of outlet temperature and additives on the formation of hollow particles in spray-dried powders. Control: ■: blend of GA/MD; Additives: ●: gelatin (1 wt%), ◆: ethanol (5 wt %), ▲: decaglycerine monolaurate (0.14 wt%).

the particles resulting in rougher surfaces. However, there were no observable differences in the appearance of particles containing one or the other of the two proteins used. The particles with only ADH were very sticky due to quick adsorption of water that destroyed the granule structures. These different external structures could be attributed to the nature of the surface crust. For example, addition of proteins may increase the porosity but may also change the flexibility of the surface, mechanical strength, evaporation of water linked to the proteins, and so on (Maa *et al.*, 1997; Landström *et al.*, 2000). Another factor potentially influencing the surface morphology could be the hydrodynamic behavior of the liquid droplet, since, upon atomization, the liquid droplets are subjected to surface turbulence and internal motion (Maa *et al.*, 1997).

The effect of outlet temperature on the formation of hollow particles in spray-dried powders is illustrated in Fig. 6.17 for various additives involved in the feed liquid (Yoshii *et al.*, 2006). The percentage of hollow particles increases linearly with the increase in the outlet air temperature. When 0.14 wt% of surfactant (HLB 10) is added to the GA/MD solution, the percentage of hollow particles is the highest, reaching about 87% at an outlet temperature of 135 °C. This phenomenon might be related to bubble formation in the sprayed droplets. High percentages of hollow particles are also obtained by the addition of small amounts of ethanol or gelatin. Gelatin is an enhancer of film formation. The film-forming property might promote the expansion of the spray droplets.

6.2.7
Particles Obtained in Freeze Spray Drying

Freeze spray drying is applied to substances with otherwise very sticky surfaces, as in the food industry, or to enable the formation of very porous structures with excellent

instant properties. In any case, the process is extremely protective and allows the maintenance of biological activities, even of very sensitive proteins like vaccines (Garmise, 2007) and bacteria, enzymes or peptides. Further protection of sensitive biopharmaceuticals is provided by additives, such as for example, mannite, trehalose or glycine (Constantino *et al.*, 2001), The respective excipients must be added to hygroscopic materials also for various applications in the food industry. The process is well suited to the formation of particles which are porous and relatively large in comparison to the original droplets, but, nevertheless, still have a small aerodynamic diameter (<5 μm), as required for pulmonal and respiratorial treatment (Wang *et al.*, 2006).

The spray is usually introduced into a cooled chamber held either at low pressure ($P < 1$ mbar) or at atmospheric pressure, then operated with a carrier gas (Heldmann, 1974; Mumenthaler, 2000). The cooling and freezing can be achieved by the cold gas or by spraying the droplets into a bath of liquid nitrogen. The fast solidification of the liquid matrix with a high nucleation rate of solvent crystals gives rise to very little de-mixing or segregation of the dissolved matter within the liquid. Therefore, a very porous and fine structure forms from the dissolved matter as soon as the solvent (most of the time water) is evaporated below the triple point (sublimation) in a second step. The sublimation process is, due to the low vapor pressure, very slow and usually needs hours to days, depending on the process. In this context, the atmospheric carrier gas technology has the advantage of being faster than the low pressure process. Figure 6.18 shows a typical particle obtained from 10 wt% solution of mannite in water in a laboratory device. The droplets were first captured and frozen in a bath of liquid nitrogen. Subsequently, the final water sublimation step was performed on trays at $T = -25\,^{\circ}C$ under a vapor pressure of $P < 1$ mbar.

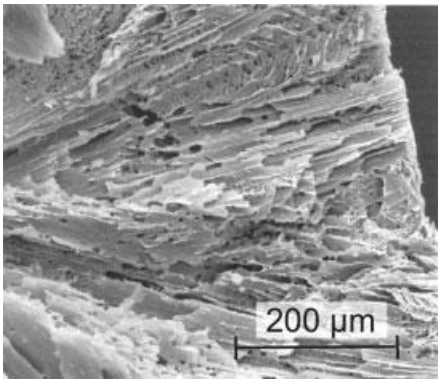

Fig. 6.18 SEM picture of structures close to the surface of a 2 mm particle formed from a 10 wt% solution of mannite in water. The solution was dripped into a bath of liquid nitrogen, suddenly frozen and dried afterwards under vacuum. The thin, lamella-like structures of the solid are formed due to the rapid crystallization of the solvent (water). The water crystals were removed by sublimation.

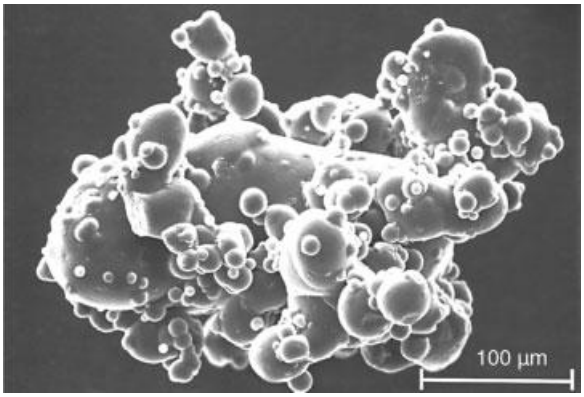

Fig. 6.19 SEM picture of agglomerated full milk particle obtained from integrated fluidized bed (FSD-System, by courtesy of GEA Niro Process Engineering, Søborg, Denmark).

6.2.8
Particles Formed in Integrated Fluidized Beds

Spray dryers of special design incorporate a fluidized bed at the bottom of the dryer. This technology allows the formation of very porous and coarse grained material with excellent instant properties, as described in Masters (1991), Herbener (1987). The process is applied to many dairy products as well as to industrial products such as pigments, where instant properties are desired. The grains consist of primary particles in the size range 50 to 200 µm first formed in the upper part of the tower. These primary, spray-dried particles stick together and are agglomerated to larger grains, typically in the size range 0.5 to 3 mm, in the fluidized bed part of the equipment. The final product shows the morphology of more or less loose agglomerates, see Fig. 6.19. Favorable conditions for agglomeration in the fluidized bed (for example, a high residual moisture after the spray dryer compartment) have been discussed by, for example, Palzer (2005).

6.3
Retention of Flavor in Spray-Dried Food Products

6.3.1
General Remarks on Microencapsulation

Microencapsulating technology has undergone a remarkable development in the past three decades and penetrated widely into daily life. As the application of microencapsulation diversifies into various fields, one finds a great number of products that rely on this technology to provide their respective unique attributes. Microencapsulation enables the capture of a core material in a shell or coating for controlled release. This can be of great advantage in the food industry, leading to

products that fulfill various purchase criteria and are, thus, highly competitive on the market. For example, microcapsulation can provide protection against degrading reactions and prevent the loss of flavor. It can also be used to control the release of flavors during food processing and storage. Microencapsulated products can be divided into five main categories: flavorings, vitamins and minerals, oils and fats (such as ω-3s and 6s), herbs and bio-actives, and other food ingredients (Barbosa-Cánovas *et al.*, 2005; Reineccius, 2005). Flavor is one of the most important factors of food quality and acceptability.

Microencapsulation of flavor is the technology of enclosing flavor compounds (core materials) in a carrier matrix. According to the concept of glass transition, dehydrated food can be considered as an amorphous or metastable solid, which is normally used as a carrier matrix. The encapsulation is useful for improving the chemical stability of flavor compounds, controlling the release of flavor compounds from microencapsulated flavor products, providing a free flowing powder with improved handling properties, and protecting the physical properties of volatile flavor.

The significance and main objective of flavor encapsulation is, therefore, to improve the stability during storage and to modify the release characteristics of the encapsulated flavor during food processing and during consumption. Encapsulation of flavor in a powder leads to a decrease in the water activity of the powder, resulting in reduced bioavailability of water inside the matrix of the powder. In addition, the reduced reactivity and mobility of the flavor prevent adverse effects such as evaporation and oxidation of flavors. Regarding the powder properties, the lowered moisture content is connected to an increase in the glass transition temperature of the matrix composing the powder. The fact that the mobility and chemical reactivity of the flavor inside the matrix increase exponentially with the moisture content and temperature shows the importance of the glass transition temperature of the matrix (Ubbink and Schoonman, 2003).

Various techniques are used for transforming liquid food flavor into the powder form (Shahidi and Han, 1993; King, 1995b; Gibbs *et al.*, 1999). The traditional, commercially available processes are spray drying, freeze-drying, fluidization drying, extrusion, the air suspension method, molecular encapsulation and coacervation. The former four methods are also called "glass encapsulation," since all these techniques use water-soluble carbohydrates in the amorphous glassy state as the encapsulation matrix, and encapsulation in these amorphous carbohydrate glasses is the operating principle (Ubbink and Schoonman, 2003). The molecular encapsulation primarily uses cyclodextrins as the encapsulant, in the molecular cavity of which flavor can be entrapped as an inclusion complex. Recently, more sophisticated techniques have been developed, such as the use of super critical carbon dioxide, crystal transformation and adsorption in the porous carbohydrates.

Among the various encapsulation methods, spray drying is the most widely used to produce flavor powders from food flavor emulsions (Reineccius, 1988). Spray drying is often regarded as a "harsh" drying method, due to the high temperature of the drying gas, but it has the key advantages of being relatively simple and suitable for continuous operation.

After the drying process, the food powder of low moisture content and, usually, glassy state is stored at room temperature. In these glassy states, flavor release and the stability of flavor depend on kinetics rather than on thermodynamic mechanisms. The respective kinetics correlates with and can be predicted from the glass transition temperature of the carrier materials. Plasticization by water absorption under conditions of high humidity may cause reduction of the glass transition temperature below room temperature. Then, the structural change in the wall material leads to collapse of the food powder, resulting in flavor release from the rubber state of the carrier matrices (Ubbink and Schoonman, 2003).

In the following sections, encapsulation of flavor by means of spray drying will be discussed. We will focus on flavor retention during spray drying, stability of the encapsulated flavor on the basis of emulsion properties, and on the release and oxidation rates in the spray-dried powder.

6.3.2
Encapsulation of Flavor by Spray Drying

6.3.2.1 Theory and Mechanism

In the case of spray drying of liquid food, the content of flavor in the powder is often an important evaluation factor of the product. Since high-temperature air is used as the drying medium, one would expect that a large amount of flavor could be lost during the drying process. In practice, over 90% of the water is evaporated, but yet relatively high amounts of volatile flavors are retained, when optimal drying conditions are followed. The question is: Why can we get flavor compounds in the powder, although most of these compounds are highly volatile with respect to water and could be easily lost during drying? The reason for the unexpectedly good retention of volatiles has been the subject of substantial research since about 1970. To summarize the results of this research, one should distinguish between the two main kinds of liquid food flavors, namely hydrophilic and hydrophobic species. The mechanisms of flavor encapsulation observed in drying processes depend on the type of flavor.

6.3.2.2 Microencapsulation of Hydrophilic Flavors

For hydrophilic flavors, like alcohol and acetone, the accepted explanation for good flavor retention was given by the "selective diffusion theory" (Thijssen and Rulkens, 1968; Coumans *et al.*, 1994; King, 1995a). The retention of the volatile compounds in spray-dried foods is considerably higher than would be predicted from equilibrium considerations alone (Bomben *et al.*, 1973), because of the rate-limiting effect of liquid phase diffusion to the surface of the droplet. In food materials containing sugars and/or polymers, the reduction of the water content increases the glass transition temperature and the resulting amorphous matrix is impermeable to organic compounds. Permeability to water, however, remains finite. As Thijssen and Rulkens (1968) noted, the water concentration at the droplet surface decreases with the progress of drying, then the diffusivities of the flavor components decrease by several orders of magnitude – more sharply than that of water. While

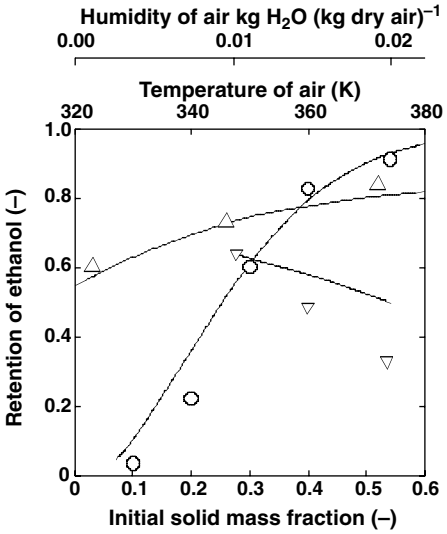

Fig. 6.20 Retention of ethanol in a single suspended droplet dried in hot air; ○: Retention of ethanol vs. initial solids (maltodextrin) mass fraction (air temperature: 323 K, velocity of air: 1.15 m s^{-1}, humidity of air: 0.008 kg H_2O (kg dry air)$^{-1}$); △: retention of ethanol vs. air temperature (initial solids mass fraction: 0.3, velocity of air: 1.2 m s^{-1}, humidity of air: 0.008 kg H_2O (kg dry air)$^{-1}$); ▽: retention of ethanol vs. air humidity (initial solids mass fraction: 0.3, velocity of air: 1.15 m s^{-1}, air temperature: 323 K). Solid curves are the results calculated on the basis of the selective diffusion theory.

water continues to permeate at a significant rate through the amorphous film, the flavors diffuse into the film at a negligible rate. Therefore, the dry surface acts as a semi-permeable membrane, permitting the continued loss of water (evaporation), but efficiently retaining (or trapping) organic flavor molecules. The essential background of this phenomenon is that the diffusion coefficients of other substances become much less than that of water above some dissolved solids content.

The selective diffusion theory has been well formulated mathematically and solved by numerical calculations. On the basis of such calculations, flavor retention during spray drying increases with the increase in solids content in the feed, inlet gas temperature and inlet gas flow rate, as well as with the decrease in inlet gas humidity, see Fig. 6.20. All of these conditions favor the early formation of a dry skin on the surface of the droplet (Furuta *et al.*, 1984).

6.3.2.3 Spray Drying of Emulsified Hydrophobic Flavors

In spray drying of hydrophobic flavors, the flavor must be emulsified into an oil/water (O/W) type emulsion in an aqueous solution of carbohydrate carrier material. The emulsion liquid is pumped through an atomizer and sprayed into a high temperature chamber. The mechanism to retain hydrophobic flavor can be explained in analogy to the case of hydrophilic flavor (Fig. 6.21). Selection of a suitable carrier material (carbohydrate) is an important initial step in spray drying, since the carrier materials

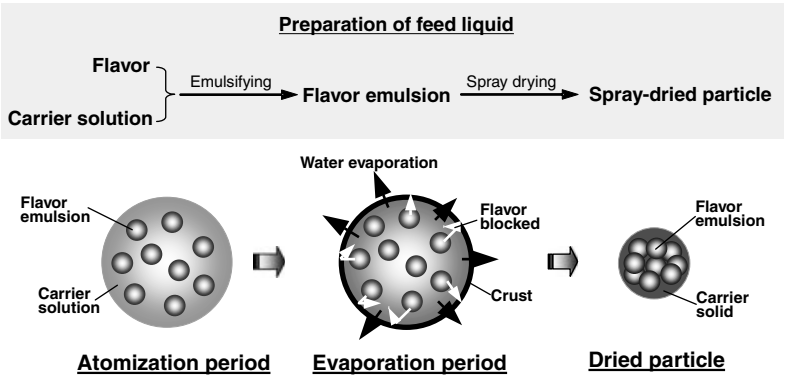

Fig. 6.21 Spray-drying scheme of emulsified flavor solution: First, the hydrophobic flavor has to be emulsified into an O/W emulsion; then, the emulsion liquid is pumped through an atomizer and sprayed into a high temperature chamber.

have an influence on the emulsion stability before drying, the flowability of spray-dried particles and the shelf-life of the powder. The ideal carrier material should possess good emulsifying properties and film-forming characteristics; it should have low viscosity even in highly concentrated solutions, exhibit low hygroscopicity, and release easily the encapsulated flavor during the reconstitution of the food product (Ubbink and Schoonman, 2003). The main types of capsule wall materials are carbohydrates (starch, maltodextrins, corn sirup solids, cyclodextrins), cellulose esters and ethers (carboxymethylcellulose, methylcellulose, ethylcellulose), gums (gum acacia, agar, sodium alginate), lipids (wax, paraffin, fats, oils), and proteins (gelatin, soy protein, whey protein).

6.3.2.4 Factors Affecting the Retention of Emulsified Hydrophobic Flavors During Spray Drying

Solids Content of Feed Solution The most important factor determining the retention of volatiles during drying is the feed solids content (Sivetz and Foote, 1963; Menting and Hoogstad, 1967; Reineccius and Coulter, 1969; Menting *et al.*, 1970; Rulkens and Thijssen, 1972; Rosenberg *et al.*, 1990; Coumans *et al.*, 1994; Liu *et al.*, 2001; Soottitantawat, 2005). A high solids content of the feed is expected to increase the retention during drying, primarily by enhancing the formation of a semi-permeable membrane on the drying particle surface. The strong dependence of flavor retention on the feed solids content is readily apparent. However, different results exist concerning the details and limits of the mentioned trend. Some researchers have suggested that one should use the highest feed solids content possible, and observed that an increase in solids content resulted in a continuous increase in volatiles retention (Rosenberg *et al.*, 1990; Sankarikutty *et al.*, 1988; Leahy *et al.*, 1983; McNamee *et al.*, 2001). On the other hand, other works have reported that each encapsulating material has a characteristic optimum concentration for maximum retention (Bhandari *et al.*, 1992; Reineccius and Bangs, 1985; Ré, 1998).

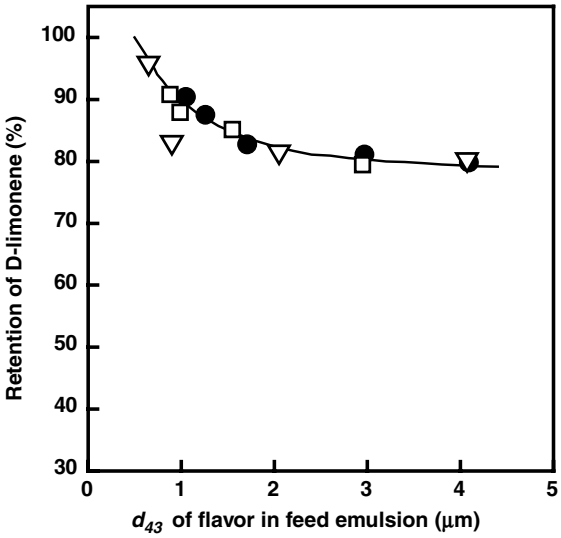

Fig. 6.22 Effect of feed emulsion droplet size d_{43} on the retention of D-limonene during spray drying (Carrier materials: ● blend of GA-MD, □ blend of SSPS-MD, ▽ blend of HI-CAP® 100-MD).

Emulsion Drop Size The influence of the feed emulsion droplet size on the retention of D-limonene during spray drying is illustrated in Fig. 6.22. For all combinations of the carrier solid, an increase in the mean diameter of the emulsion droplets in the feed resulted in decreasing retention of D-limonene. Flavor retention markedly decreased, especially for emulsion drops with mean sizes in the range 0.5–2.0 μm (Soottitantawat *et al.*, 2003). This implies that a fine emulsion is stable during both the atomization and spray drying. It also indicates that for the proper carrier materials, the emulsion droplet size is a market factor for the retention of flavor (Risch and Reineccius, 1988). It might be suspected that the large droplets would be changed to smaller droplet size during the atomization. Droplet size distribution curves before and after atomization are shown in Fig. 6.23a for an initially coarse emulsion embedded in a blend of GA and MD as the carrier material. The distribution of the emulsion drop size in the spray-dried powder (reconstituted emulsion) is also shown in the figure. The distribution curve after atomization is shifted towards a smaller size whereas the distribution of the emulsion droplet size after drying appears unchanged compared with the droplet size distribution after atomization. This implies that the larger emulsion droplets would be sheared into smaller droplets because of the large shear rate and the turbulence in the thin liquid film on the surface of the rotating atomizer. Some of the sheared droplets would then be broken and evaporated during atomization. These results give a reasonable explanation for the greater loss of flavor from the larger emulsion droplets during spray drying, as shown in Fig. 6.22. On the other hand, the distribution curves of the fine emulsion are almost unchanged before and after atomization, as shown in Fig. 6.23b. This implies that the fine emulsion

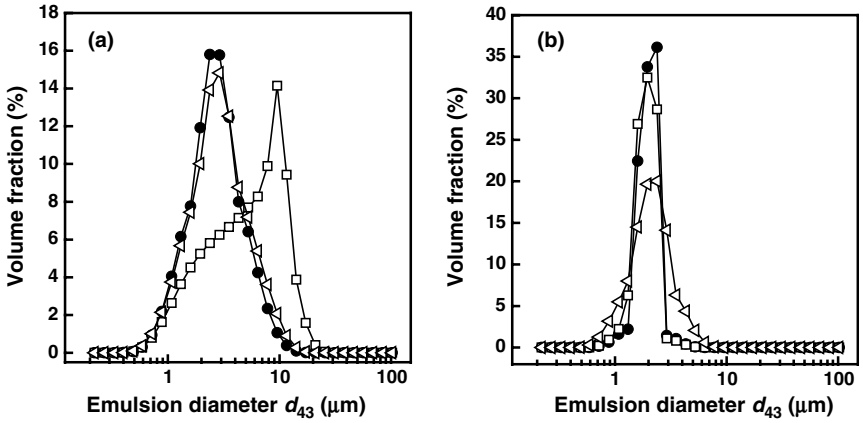

Fig. 6.23 Changes in distribution of emulsion droplet size before and after the atomization with a rotary atomizer. (a) Coarse emulsion in feed liquid, (b) fine emulsion in feed liquid. Carrier material is a blend of GA and MD, flavor is D-limonene. □ Feed emulsion, ● Emulsion after atomization, ◁ Reconstitute emulsion encapsulated in spray-dried powder.

droplets experienced much less breakage during atomization than the coarse emulsion droplets, thus resulting in higher retention.

Type of Flavor (Solubility of Flavor) The retention of flavor depends not only on the emulsion drop size, but also on the solubility of the flavor ingredient. Several esters in gum arabic encapsulation were studied with regard to their retention by Rosenberg *et al.* (1990). The retention of partially water-soluble esters, such as ethyl propionate and ethyl butyrate, was less good than the retention of esters having lower solubility (ethyl caproate). Soottitantawat *et al.* (2003) also reported this trend, which is illustrated in Fig. 6.24, in agreement with further similar findings by Liu *et al.* (2001). Higher retention of D-limonene (insoluble flavor) was observed compared to ethyl butyrate and ethyl propionate. It is quite interesting to see, in Fig. 6.24, that more water-soluble volatiles have an optimum emulsion drop size for flavor retention. The increased loss of the esters at small emulsion sizes could be due to the larger surface areas of the fine emulsions. The increase in surface area of emulsion droplets would result in accelerated dissolution of the flavor in the carrier solution and loss from its surface during drying (Soottitantawat *et al.*, 2003).

Flavor Load Higher flavor loading generally results in poorer flavor retention (Rulkens and Thijssen, 1972; Rosenberg *et al.*, 1990; Reineccius and Coulter, 1969). This is anticipated since higher loading results in greater proportions of volatiles close to the drying surface, thereby shortening the diffusion length to the particle interface. Because higher volatile loading leads to greater losses, most volatile flavorings are dried at a carrier solids to flavor mass ratio of 4 to 1 (Bhandari *et al.*, 1992; Risch, 1995; McNamee *et al.*, 1998; Ré, 1998; Gibbs *et al.*, 1999). This ratio has been reported to be optimal for encapsulating materials like gum arabic and for other carbohydrate derivatives (Reineccius, 1988).

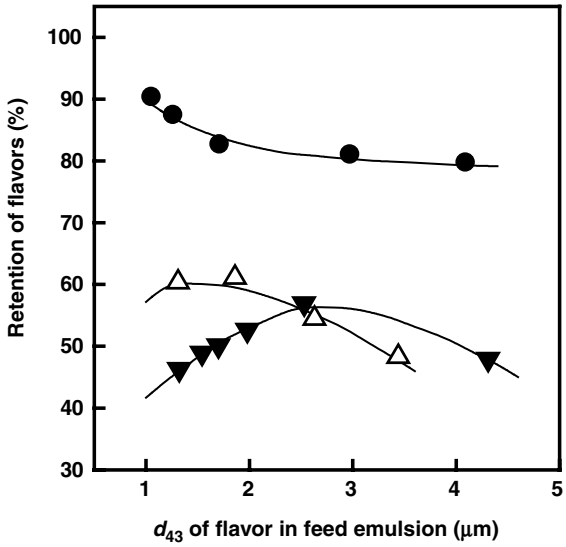

Fig. 6.24 Different effects of the volume-averaged mean diameter d_{43} of emulsion droplets in the feed liquid on the retention of flavors for different flavor solubilities. The retention of D-limonene (●) decreases with the increase in emulsion droplet size. Ethyl butyrate (△) and ethyl propionate (▼), on the other hand, have an optimum emulsion droplet size for flavor retention. The wall material was a blend of GA and MD.

6.3.2.5 **Stickiness of the Spray-Dried Powder**

The stickiness and subsequent adhesion of particles on the dryer surface is one of the serious problems encountered in the spray drying of sugar-rich foods (Bhandari and Howes, 1999; Adhikari *et al.*, 2005). Therefore, stickiness is an important side-condition for aroma encapsulation or, in general, for spray drying of food products. The deposition of the powder inside the dryer chamber causes unfavorable agglomeration and leads to lower product yield and performance of the spray dryer. The stickiness of the powder has a significant impact on whether a liquid food can be successfully spray dried to produce free-flowing powder. In recent years, it has been well recognized that the stickiness is closely related to the state changes of the carrier materials (Levine and Slade, 1986; Roos, 2003). The state change is a secondary one and observed at a particular temperature called the "glass transition temperature." The glass transition temperature exhibits strong dependence on the moisture content (Ubbink and Schoonman, 2003); the lower the moisture content, the higher the glass transition temperature. As mentioned before, the atomized fine droplets contact with hot and dry air, resulting in sudden formation of the low-moisture carbohydrate membrane, called "case hardening." Since the surface water of the droplet is evaporated very quickly, the low-moisture film forms in an amorphous state, which has a higher glass transition temperature than the original matrix material. Therefore, the spray drying process can be considered as a state transition from liquid to amorphous solid with a higher glass transition temperature.

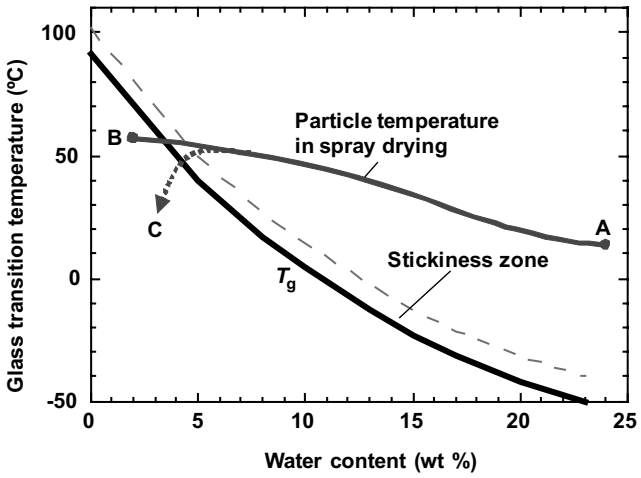

Fig. 6.25 Hypothetical history of the relationship between particle water content and particle temperature for successful spray drying of lactose-rich dairy powders.

Formation of the glassy particle surface is the basic requirement for successful spray drying, since such solidified surfaces avoid agglomeration between contacting particles or adhesion on the inner surface of the dryer (Roos, 1995). Therefore, the relationship between temperature and water content of the particle should be appropriately controlled and adjusted according to the relationship between the glass transition and the water content. Figure 6.25 illustrates schematically the relationship between glass transition temperature and water content for lactose. The same plot shows the sticky region located between the glass transition and the stickiness line (dotted line), which also depends on the temperature and water content (Roos, 2003). Commonly, the stickiness line is estimated to be by 10–20 K higher than the T_g-line (Bhandari and Howes, 1999). During spray drying, the relationship between the particle temperature and the water content may change from point A to B or C along some hypothetical line. To avoid particle agglomeration and adhesion to the dryer wall, the particle moisture content should be lowered so as to increase the particle glass transition temperature. Suppressing the final particle temperature might be an alternative technique to avoid undesired results (Roos, 2003; Adhikari *et al.*, 2005).

6.3.3 Release and Oxidation of the Encapsulated Flavor During Storage

6.3.3.1 Influence of Glass Temperature on the Storage Stability of the Encapsulated Flavor

The objectives of micro-encapsulation of food liquid flavors or oils are primarily to provide dry and free-flowing powders, to provide protection against the degrading reaction, and to prevent the loss of flavors during food processing and storage.

Additionally, the encapsulation gives some benefits of controlled release of flavor and retardation of oxidation of oil. These functional properties of encapsulated flavors and oils are closely related to the structure of the carrier matrix materials. Several physico-chemical properties of the carrier matrix (commonly a carbohydrate) are directly or indirectly functions of the glass transition temperature of the amorphous glass. The glass transition temperature (the glass–rubber transition temperature) is, as already discussed, a property of amorphous materials (carbohydrates and proteins). In the amorphous state, the encapsulation carrier matrix is physically stable and does not undergo any significant structural changes. If the temperature and water content increase, the rheological property of the carrier matrix changes from the glassy, that is, brittle, state to the rubbery or visco-elastic state, causing some undesirable structural variations. The glass transition temperature is – as previously mentioned and also pointed out in several other chapters of the present volume – drastically altered with the water content; higher water content corresponds to lower glass transition temperatures. The glass transition temperature also depends on the molecular weight of the carrier material. A decrease in the average molecular weight of the carbohydrate leads to a reduction in the glass transition temperature.

In general, the rotational and vibrational motions of molecules are limited in the amorphous glass state. In the rubbery state, large-scale molecular motion, such as translational motion, is possible (Ubbink and Schoonman, 2003). Therefore, the encapsulated flavor or oil exists stably in the amorphous glassy state, but in the rubbery state some deterioration takes place. Since amorphous states are non-equilibrium states, thermodynamic driving forces tend to shift the amorphous state into a more stable crystalline state, resulting in time-dependent crystallization, solidification of powders, and caking.

6.3.3.2 Release of Flavor from Spray-Dried Powder During Storage

Mathematical Modeling of Flavor Release The analysis of flavor release from spray-dried powder is complex and difficult because the phenomena influencing the release – namely diffusion of flavor and water, and oxidation of flavor – are intrinsically combined and overlap with each other. Since the diffusion of molecules in a low moisture carbohydrate matrix is strongly dependent on the glass transition temperature of the matrix (Roos, 1995), the release and oxidation of the encapsulated flavors have been related to the structural changes in the matrix, such as collapse and crystallization (Labrousse *et al.*, 1992). A better understanding of the effect of storage relative humidity on the properties of capsule matrices would be useful in the quality control and applications of these powders (Whorton and Reineccius, 1995; Gunning *et al.*, 1999; Beristain *et al.*, 2002). A simple correlation was proposed for the correlation of retention with the release time in the course of the storage of spray-dried ethyl-n-butyrate powder (Yoshii *et al.*, 2001):

$$R = \exp[-(k_R t)^n] \tag{6.6}$$

Here R is the retention of flavor in the powder, t is the storage time, k_R is the release rate constant, and n is a parameter representing the release mechanism. Equation 6.6 is also called Avrami's equation and resembles the Weibull distribution function,

which has been successfully applied to describe the shelf life failure (Gacular and Kubala, 1975). The release mechanism of flavor can be simply characterized by the value of n used in Eq. 6.6. Zero order release occurs when the core ingredient is a pure material (flavor) and penetrates through the wall of a reservoir microcapsule (carbohydrate) (Karel and Langer, 1988). Half order release ($n \approx 0.5$) generally occurs when the flavor diffusion inside the carrier matrix primarily governs the process. The release is of first order when the core material is actually a solution. Finally, in the case of $n > 1$, an induction period followed by a burst of flavor emulsion can be observed. Note, however, that the described classification of release mechanisms is valid for a given single microcapsule. A mixture of microcapsules usually includes a distribution of capsules varying in size and wall thickness. Since any spray-dried powder produced from an emulsion is essentially such a mixture of microcapsules with variations in their properties, the parameter n in Eq. 6.6 varies depending on the properties of the powder. Equation 6.6 is essentially analogous to the equation of Kohlraush–Williams–Watts (KWW). This relationship can be expressed as (Williams and Watts, 1970)

$$M = M_0 \exp[(-t/\tau)^{\beta}], \quad R = M/M_0 \tag{6.7a, b}$$

where $M(t)$ corresponds to the residual amount of flavor in the powder, M_0 to the initial mass of the flavor, τ is the relaxation time which corresponds to the inverse of the release rate of the flavor, and β is the relaxation constant. Equation 6.7a, was originally proposed to express the relaxation phenomena in a polymer. The relaxation constant β represents the breadth of the energy distribution in polymer relaxation phenomena; $\beta = 1$ means simple relaxation, whereas smaller values of β mean a larger width of the energy distribution. As already mentioned, spray-dried powder consists of various particles having different release characteristics. Consequently, the total release behavior may be considered as the sum of many KWW relaxation equations valid for individual particles, i, or classes of particles:

$$M = \sum M_{0,i} \exp\left[(-t/\tau)^{\beta_i}\right] \tag{6.8}$$

The release of flavor from the spray-dried powder during storage is recognized as a kind of relaxation phenomenon in an amorphous glass, inside which emulsion droplets of different sizes are distributed. Therefore, it should be possible to develop alternative correlation equations of flavor release from a statistical perspective. Considering the distribution of activation energy for the rate constants (Kawamura *et al.*, 1981), the following equation was developed for the correlation of the complicated time-dependent phenomena:

$$R = \frac{C}{C_0} = \frac{RT}{\sqrt{2\pi\sigma}} \int_{-\infty}^{+\infty} \exp\left(- \frac{R^2 T^2 \left(\ln k_1 - \ln k_{1,0}\right)^2}{2\sigma^2} \right) \exp(-k_1 t) d(\ln k_1) \tag{6.9}$$

with

$$k_1 = \frac{kT}{h} \exp\left(-\frac{\Delta G}{RT}\right) \tag{6.10}$$

Here C is the flavor concentration in the stored spray-dried powder, C_0 is the initial flavor concentration, $k_{1,0}$ is the initial release rate constant, ΔG is the activation energy of flavor release, k is Boltzmann's constant and h is Planck's constant. Equation 6.9 was originally developed to express the inactivation kinetics of α-chymotrypsin and glucoamylase covalently bound to a water-insoluble support in an aqueous system (Kawamura *et al.*, 1981). Equation 6.9 was applied to express the oxidation kinetics of fish oil (EPA) in linoleic acid powder, based on the assumption that the free energy of activation ΔG follows a Gaussian distribution with the standard deviation σ (Yoshii *et al.*, 2003; Ishido *et al.*, 2002, 2003).

The abovementioned three equations are equivalent to the perspective of simulating the flavor release from spray-dried powder. All of the parameters – namely n in Avrami's equation, β in the KWW-equation, and a Gaussian distribution of ΔG with the standard deviation σ in Eq. 6.9 – can be understood as a consequence of the activation energy distribution of the release rate.

Release Rate of Flavor At Various Relative Humidities and Temperatures The release behavior of flavors not only varies with the relative humidity, but also with the composition of the carrier materials. The combination of moisture and temperature strongly influences the degree of plasticization of the carrier material during storage, thereby governing the rates of flavor loss.

A typical example of the release kinetics of encapsulated flavor in spray-dried powder is illustrated in Fig. 6.26. The plot shows the residual mass fraction of D-limonene in powder stored at 50 °C at 23%, 51%, 75%, and 96% relative humidity (RH) according to measurements by Soottitantawat *et al.* (2004a). In all cases, a blend of GA and MD was the capsule matrix. The relative humidity greatly affects the

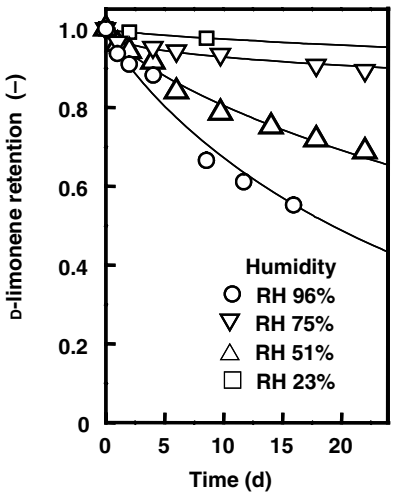

Fig. 6.26 Release kinetics of D-limonene encapsulated in spray-dried powders stored at various relative humidities and at 50 °C. Carrier material is a blend of GA and MD. Relative humidity (RH): □ 23%, △ 51%, ▽ 75%, ○ 96%.

release rate of D-limonene, but the relationship is not simple. Considering only 23% and 96% RH the release of D-limonene increases with increasing RH. However, when comparing the results of 51% and 75% RH, one can see that the release of D-limonene at 51% RH is higher than that observed at 75% RH. These results prove that the release of D-limonene is closely related at least to the water activity of the powder (Yoshii *et al.*, 2001; Levi and Karel, 1995). The loss of D-limonene during storage may be caused by two mechanisms: diffusion through the matrix of the carrier material and oxidation. However, the loss by oxidation was at most 5–6% of the initial D-limonene content. Therefore, the observed loss of D-limonene may be considered to result mainly from release by diffusion (Whorton and Reineccius, 1995). To evaluate the release rate constant of D-limonene, Eq. 6.6 was applied to the measured release kinetics, resulting in the solid curves in Fig. 6.26. These solid curves show that Eq. 6.6 can correlate successfully the release curves of D-limonene and the release rate constant k_R can be estimated as a function of RH (Soottitantawat *et al.*, 2004a). The same correlation was also applied to various other carrier materials. Figure 6.27 shows the resulting release rate constant k_R in dependence on the water activity α_w of the carrier matrices. In brief, the release rate constant k_R first increases with increasing α_w, followed by a decrease at around $\alpha_w = 0.70$. At a still higher α_w, the release rate constant tends to increase again because the powder matrices are destroyed. The variation pattern of k_R against α_w is very similar irrespective of the kind of carrier material. A similar phenomenon was observed in the study of the equilibrium head space volatile concentration of roasted coffees as a function of water

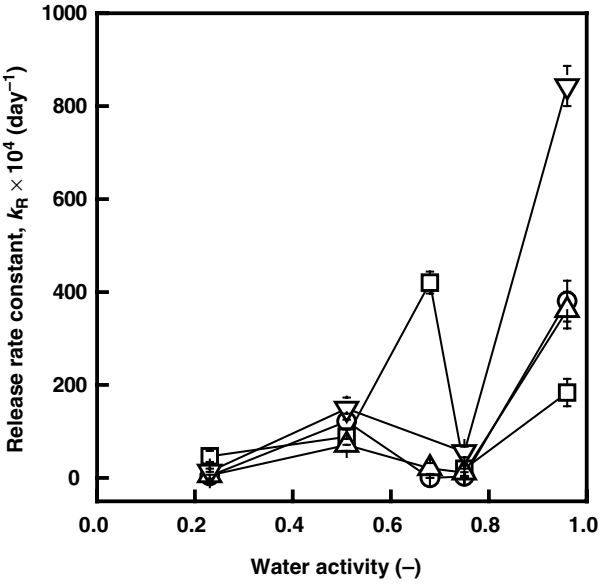

Fig. 6.27 The relationship between the release rate constants k_R and the water activity of the carrier matrices α_w at 50 °C; Carrier material: ○ blend of GA-MD, □ blend of SSPS-MD, ▽ blend of HI-CAP® 100-MD, △ HI-CAP® 100. The error bars indicate 95% confidence levels.

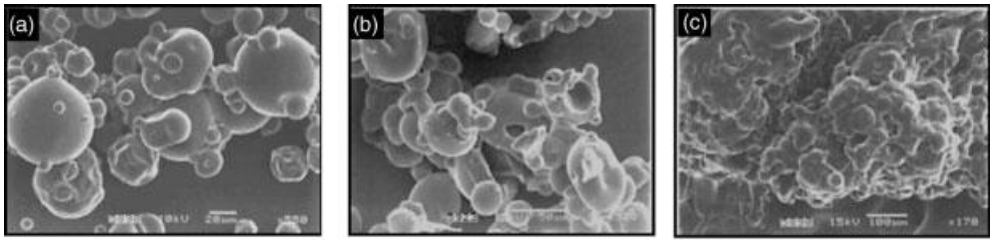

Fig. 6.28 Outer structural changes during storage at 50 °C of spray-dried powder produced in the form of wall capsules from the blend GA-MD; (a) storage at 23% RH for 1 w, (b) storage at 51% RH for 1 w, (c) storage at 75% RH for 1 d.

activity. The volatile concentrations were found to be low at very low and at high water activities. They were highest at intermediate water activity in the range 0.25–0.35 for the light and medium-roasted coffees and at about 0.7 for the dark-roasted coffee (Anese *et al.*, 2005). The decrease in k_R between 51% and 75% RH in Fig. 6.27 corresponds to the mentioned reversal of the release curves of D-limonene in Fig. 6.26. It may be closely related to the particle matrix structure changes from amorphous glass to the rubbery state by the plasticizing effect of moisture adsorption.

In order to explain the structural changes that happen in the powder at different α_w, scanning electron microscopy (SEM) was used to observe the outer structure of the powder during storage, as shown in Fig. 6.28 (Soottitantawat *et al.*, 2004a). At a low RH ($\approx$0.23) the spray-dried particles remain in their original shape and the carrier solid seems to be still in the glassy state (Fig. 6.28a). As compared to the release rate at a water activity of 0.23, the release rate at $\alpha_w \approx 0.51$ is higher, though the structural changes cannot be observed clearly (Fig. 6.28b). This suggests that the higher mobility of D-limonene is due to the start of plasticizing of the capsule matrices. When the water activity increased further to a value of around 0.7, the powders began to be re-hydrated (Fig. 6.28c). At this stage, it may be assumed that a decrease in effective surface area resulted in a decrease in D-limonene evaporation from the surface of the powder particles. Most particles are observed to be clogged and adhering together into a paste-like mass, which indicates the rubbery state of the carrier matrices. The regime corresponds to the minimal value of k_R. At a very high α_w, the release rate increased again (Fig. 6.27). The most likely explanation is that the emulsion droplets of D-limonene in the powder are opened due to the destruction of the capsule matrices (Whorton and Reineccius, 1995).

PTR-MS as a New Methodology for Analyzing Flavor Release Recently, thanks to the pioneering work by Dronen and Reineccius (2003), proton transfer reaction mass spectrometry (PTR-MS) has been used as a rapid analysis method to measure the release time-course of flavors from spray-dried powders. The traditional equilibrium method for flavor release mentioned above is extremely time-intensive, and commonly several weeks are necessary to obtain a full release profile of the flavor from the powder. The PTR-MS method has been applied extensively to analyze the release

kinetics of volatile organic compounds from roasted and ground coffee beans. The release profiles were mathematically analyzed by means of Eq. 6.7a, to obtain the release kinetic parameters (Mateus *et al.*, 2007). The method is quite sophisticated and quickly leads to results. However, as suggested by Dronen and Reineccius (2003), comparing release profiles with those obtained by the traditional method, the disadvantage of PTR-MS is its inability to capture time-dependent phenomena (relaxation phenomena) such as the collapse and glass transition of the carrier matrices. As mentioned above, the relaxation phenomena related to the state change in the carrier matrices have a significant effect on the flavor release characteristics. However, these time-dependent phenomena cannot be detected and properly accounted for with the PTR-MS method.

6.3.3.3 Oxidation of Encapsulated Flavor During Storage

In addition to the release of flavors through the wall of the spray-dried particles, oxidation of the encapsulated flavors is also an important index of stability. Many different products form in oxidation reactions of flavor. In the case of the encapsulation of the model flavor D-limonene, limonene oxide (limonene-1, 2-epoxide) and carvone are commonly chosen as indicators of the oxidation. These products are generated together in the oxidation reaction of D-limonene (Anandaraman and Reineccius, 1986). The formation of the oxides also markedly depends on RH and increases initially during storage. During the initial period, the formation of oxides increases linearly with time, so that the apparent oxidation rate constant can be calculated on the basis of zero order kinetic reaction schemes (Anandaraman and Reineccius, 1986). However, over a longer storage time the formation rate of the mentioned oxides tends to decrease, particularly at higher RH. This might be explained by the accelerated degradation towards other oxide compounds and release of the oxides into the surroundings (Soottitantawat *et al.*, 2003). The initial oxidation rate constants (zeroth order reaction rate) k_X are plotted in Fig. 6.29 for carrier matrices consisting of GA-MD during storage at 50 °C. The changes in k_X are very similar to those of the release rate constants k_R shown in Fig. 6.27. In fact, the data for the GA-MD blend are the same (empty cycles in Fig. 6.27, full cycles in Fig. 6.29), so that they provide a basis for assessing the influence of water activity on k_X from Fig. 6.29. In this way, one can see that the oxidation rate constant k_X reaches a maximum at $\alpha_w \approx 0.5$ where the powder matrix structure begins to change from glassy to a rubbery state, and comes to a minimum at $\alpha_w \approx 0.7$.

6.3.3.4 Relaxation Process Correlation by Glass Transition Temperature

The release and the oxidation processes of the encapsulated D-limonene are closely related to the structural changes in the capsule matrices. Physico-chemical changes caused by the phase transition of carbohydrate from amorphous glass to rubbery are commonly expressed with the temperature difference between the storage temperature, T, and the glass transition temperature, T_g, of the carrier matrices, $T - T_g$. The idea is based on the fact that the viscosity (or relaxation time) of the carrier matrices follows the Williams–Landel–Ferry (WLF) equation expressed as a function of $T - T_g$ (Williams *et al.*, 1955). Therefore, the release rate constants k_R and the oxidation rate

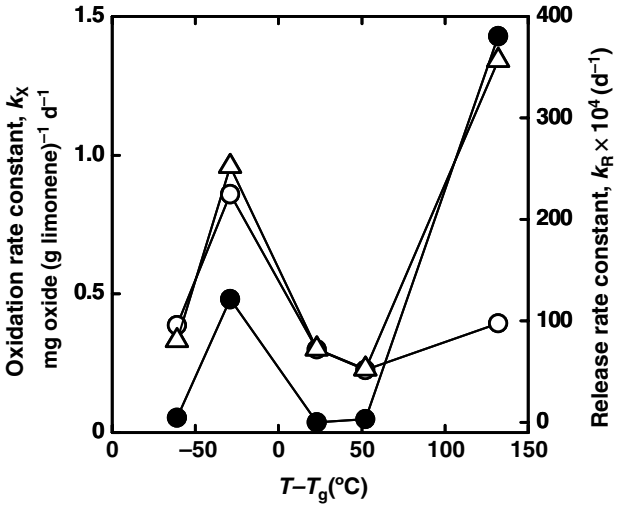

Fig. 6.29 Correlation of k_R and k_X with $T - T_g$ at $T = 50\,°C$: ● D-limonene released, ○ limonene oxide, △ carvone. Carrier material is a blend of GA and MD.

constants k_X are correlated with $T - T_g$, as shown in Fig. 6.29. The rate constants k_R and k_X increase with an increase in $T - T_g$ up to the point where $T - T_g$ becomes roughly equal to zero. This is followed by a decrease and then an increase again with increasing $T - T_g$. A high release rate near the glass transition temperature (this means at T-$T_g \cong 0$) can be explained by the increasing mobility of D-limonene and oxygen molecules. Furthermore, low release and oxidation rates are observed in the range $0 < T - T_g < 50$ K, when the powders are transformed from amorphous to a rubbery state. In this region, higher mobility of D-limonene and oxygen should occur, but at the same time, the collapse of the powders occurs, so that the particles clump and adhere together. This results in closing the pore spaces between the particles and decreasing the surface area for D-limonene evaporation and oxygen uptake. Whorton and Reineccius (1995) observed a similar behavior and defined the state of stickiness and aggregation above the glass transition temperature as the "re-encapsulation of flavor." These results imply that the release rate and the oxidation reaction rate have a mutually close connection to T_g. The rubbery state and collapse of carrier matrices are associated with greater stability as compared to the glassy state because the decrease in surface area which occurs with the aggregation of carrier matrices can restrict both the release of flavor and the uptake of oxygen from the surface to the interior of the particle (Nelson and Labuza, 1992; Labrousse *et al.*, 1992; Levi and Karel, 1995).

Figure 6.30 is a schematic picture of a spray-dried particle in a humid air environment, in which the particle can absorb water vapor, followed by a state change of the carrier matrix from amorphous into rubbery. The encapsulated flavor can easily move in the rubbery carrier matrix. At the same time, oxygen uptake into the matrix wall becomes stronger, and oxidation of the encapsulated flavor progresses. Most interestingly, around the glass transition temperature both the release

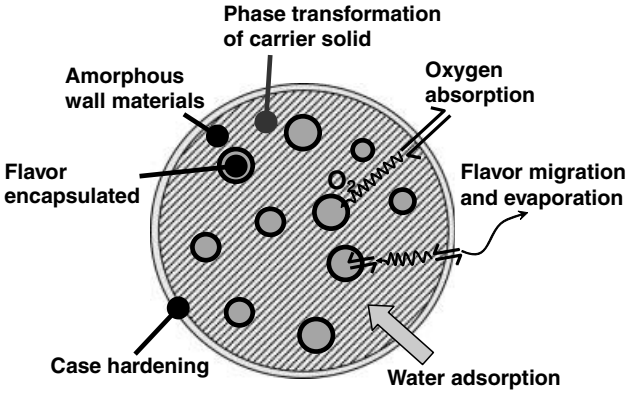

Fig. 6.30 Schematic illustration of a spray-dried particle in a humid air environment. The particle can adsorb water vapor, so that the state of the carrier matrix can change from amorphous into rubbery.

and the oxidation rates change according to nearly the same trends with $T - T_{g,}$ as shown in Fig. 6.29, indicating that the flavor diffusion and the oxygen uptake can be treated as similar processes.

6.4
Encapsulation and Microencapsulation of Enzymes and Oil by Spray Drying

6.4.1
Microencapsulation of Enzymes by Spray Drying

A biotechnologically produced molecule with therapeutic activity is commonly a protein consisting of a chain of several hundred amino acids with a complex three-dimensional structure. Protein-based drugs should remain stable for several years, maintaining the active conformation even under unfavorable conditions during transportation or storage. Freeze drying is one of the most common formulation methods of protein drugs, as discussed in detail in Chapters 3 and 4. However, freeze drying does not lead to well-defined microparticles and is a comparatively expensive and time-consuming process.

Spray drying is an attractive alternative for the preparation of solid pharmaceutical substances compared to freeze-drying. However, spray drying bears risks of product damage due to the surface-induced denaturation of biomolecules during atomization and to the subsequent drying at a high temperature of the drying gas, which can be potentially detrimental to heat-sensitive biological materials such as enzymes. Therefore, it is important to develop new formulation concepts for encapsulation and stabilization of proteins during spray drying.

Several factors may cause substantial inactivation of enzyme proteins during spray drying. Proteins are presumably exposed to high shear forces during the atomization

process. Though proper selection of atomizers is important for the reduction of the inactivation of enzymes, few studies of this subject have been made. After atomization, droplets of enzyme solution come into contact with the high temperature air, suffering from thermal stress, which can result in an irreversible structural change of the enzyme (thermal denaturation). This stress is decreased by the addition of excipients such as disaccharides. Their role during spray drying is to replace water and to form an amorphous glass, thus providing a stabilizing effect. The air temperature is obviously a significant factor in thermal stress during spray drying. Some researchers studied the thermal inactivation of several enzymes during drying by the single suspended droplet method. They suggested that most enzymes start to degrade when the droplet enters the falling rate period of drying. In industrial spray dryers, the major part of the water in the droplet evaporates almost instantaneously in the vicinity of the atomizer. The dried droplets are then surrounded by air with the still high outlet temperature until being entrapped in the cyclone. This period during the spray drying process actually corresponds to the falling rate period in drying of single droplets, where enzymes suffer from severe thermal stress, resulting in extensive enzyme denaturation. Therefore, low air temperatures must often be used, and the resulting decrease in product yield must be accepted.

Besides lowering the air temperature, the addition of some proteins or surfactants offers another way to prevent direct contact of protein materials with the high temperature air. These substances tend to distribute preferentially on the surface of the particle, thus protecting the enzyme from thermal damage. However, the effect of additives in relation to the spray drying conditions has not yet been studied extensively. In industrial spray dryers the size of the sprayed droplets is a few hundreds of micrometers. Therefore, the addition of proteins or surfactants may be one of the key techniques for the production of pharmaceutical enzymes by spray drying (Broadhead *et al.*, 1992; Giunchedi and Conte, 1995; Wendel and Çelik, 1997; Lee, 2002; Ré, 2006; Vehring, 2007).

6.4.2
Stress on Proteins During the Spray Drying Processes

Spray drying of protein solutions can result in substantial inactivation. Proteins have the tendency to denature and undergo irreversible aggregation during various steps of spray drying for various stress reasons. These reasons are shown schematically in Fig. 6.31 (Lee, 2002) and will be discussed in the following.

6.4.2.1 **Adsorption Stress**

The loss of native protein by adsorption to surfaces is problematic in biopharmaceutical applications. Proteins are able to adsorb at liquid/gas, liquid/solid and liquid/liquid interfaces due to their amphiphilic property. Adsorption stress can occur in the vessel of the feed protein solution, and at the liquid/gas interface between the sprayed droplets and the hot air. Adsorption to the vessel wall is assumed to be practically negligible, whereas the adsorption at the liquid/gas interface may lead to substantial degradation because of the strong increase in the liquid/gas

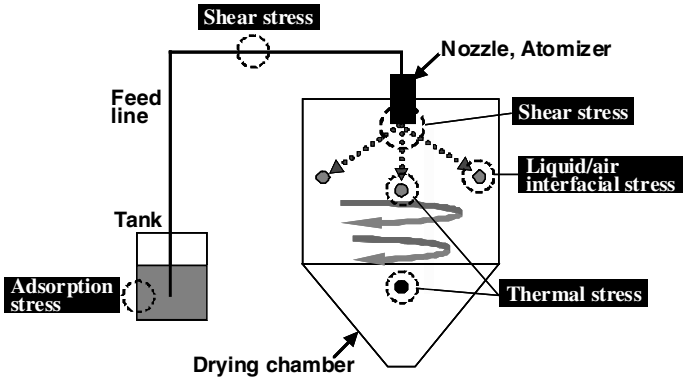

Fig. 6.31 Schematic diagram of a spray-drying system illustrating possible stresses experienced by protein solution and droplets.

interface area during atomization. Spray drying of adsorption sensitive proteins such as the recombinant human growth hormone (rhGH) has already evidenced the detrimental effect of adsorption stress (Maa *et al.*, 1997). Addition of an appropriate amount of surfactant can reduce the inactivation of protein induced by atomization (Maa *et al.*, 1997; Adler and Lee, 1999; Yoshii *et al.*, 2008). The investigation of the surface element composition of spray-dried particles by ESCA (electron spectroscopy for chemical analysis) revealed the decrease in protein content at the particle surface by addition of surfactant (Adler and Lee, 1999).

6.4.2.2 **Shear Stress**

Proteins are presumably exposed to high shear forces in the liquid feed duct, in centrifugal atomizers and, especially, in pressure nozzles during the atomization process. Soottitantawat *et al.* (2003) showed that emulsions containing large droplets are broken during atomization with a centrifugal atomizer due to the high shear force induced in the centrifugal outward flow on the rotating vane. Maa and Hsu (1996, 1997) extensively examined the effect of shear stress on the denaturation of rhGH. They concluded that the combination of shear and liquid/air interface triggered the formation of non-covalent aggregates of the protein, while shear alone did not induce significant denaturation of the protein. Addition of an appropriate amount of a surfactant to the protein solution can reduce the amount of aggregation induced by atomization.

6.4.2.3 **Thermal and Dehydration Stress**

After atomization, the protein comes into contact with the high temperature air. Proteins may denature with structural changes under thermal stress and lose their activity. This thermal stress can generate an irreversible structural change during spray drying, resulting in thermal denaturation of proteins. Therefore, excipients are often added to the feed protein solution to improve the stability in the manufacturing process and storage. Numerous studies have documented the protective effects of

excipients on the thermal degradation by means of analytical methods such as FTIR and SE-HPLC. The mechanisms of stabilization by the excipients during dehydration are supposed to be the direct interaction between excipients with the protein to protect the biostructure through hydrogen bonds, the trapping of water molecules close to the protein surface, and the entrapment of a particular protein conformation in a highly viscous amorphous glass of the excipients. These mechanisms will be further discussed in the subsequent section.

6.4.3 Protein Encapsulation Theory by Spray Drying

Encapsulation involves the incorporation of active ingredients such as flavors, enzymes, cells or other materials in small capsules. The choice of excipients for encapsulation is very important for the encapsulation efficiency and protein stability within the matrix. Applications of this technique have increased in the food and pharmaceutical industries since the encapsulated materials can be protected from moisture, heat or other extreme conditions. Thus their stability is improved and their viability maintained. Powder formation can lower the water activity of the material, the reactivity and the diffusivity of encapsulated compounds, and the diffusivity of residual water. In the food industry microencapsulation is often associated with the already discussed retention of flavor compounds during drying and storage. In pharmaceutical applications, the purpose of microencapsulation is to control the release and improve the bioavailability of active ingredients.

The exclusion of water from the environment of a protein may provide resistance to chemical modification of the protein structure during processing and storage. Processes such as freeze-drying and spray drying have been employed to prepare solid-state dosage forms of pharmaceutical proteins with vastly reduced water content. Several theories of protein encapsulation in glassy materials have been proposed based on the three considerations mentioned in Section 6.4.2.3:

- The first is the "water replacement hypothesis" proposed by Crowe *et al.* (1984) for the preservation of proteins in the dried state. According to this hypothesis, biostructures are protected by means of hydrogen bonds resulting from their direct interaction with stabilizer molecules. Certain physiological solutes "replace" the water lost around polar residues of proteins from the primary hydration shell during dehydration. As shown in Fig. 6.32, the wall material, in this case trehalose, is acting as a substitute for hydration water molecules. Carpenter and Crowe (1984) suggested that some of the hydroxy groups of sugars form hydrogen bonds with the polar residues of proteins. Sugars such as trehalose are often used in pharmaceutical, food and biomedical applications to prepare glassy matrices for long-term storage of biological materials.
- Secondly, the "water layer hypothesis" proposes that the stabilization of proteins is achieved by the trapping of water molecules close to the biomolecular surface (Belton and Gill, 1994). The protein stabilization conferred by the excipients during dehydration is brought about primarily by these excipients substituting for water molecules on the surface of the protein.

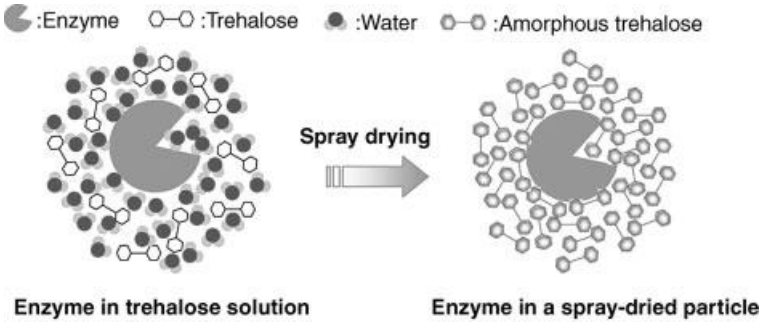

Fig. 6.32 Concept of the "water replacement hypothesis.".

- The third hypothesis is called the "glass entrapment hypothesis" which proposes stabilization through entrapment of a particular biomolecular conformation in a high viscosity glass (Ansari *et al.*, 1992). Franks *et al.* (1994) suggested the similar "glass state theory" explaining the glass formation to be responsible for the stabilization of proteins. The molecular mobility of the protein-containing system is greatly limited by trapping protein molecules in a glassy matrix. As a consequence the rates of diffusion-controlled reactions, including protein unfolding, protein aggregation and chemical degradation, are reduced.

6.4.4 Spray Drying of Protein Solutions

6.4.4.1 Drying of a Single Suspended Droplet

Yamamoto and Sano (1992, 1994) studied the thermal inactivation of several enzymes during drying of a single suspended droplet. The droplet had a diameter of 1.5 to 2 mm and contained β-galactosidase, glucose oxidase, or alkali phosphatase. It was suspended on a fine glass filament and dried in an air stream. The time course of enzyme inactivation was obtained during drying at constant drying conditions (temperature, humidity, velocity, etc.). The same technique was previously applied to investigate the time profile of lipoxygenase inactivation during drying (Liou, 1982). The kinetic model for the enzymatic inactivation reaction was obtained from separate experiments conducted at various temperatures and relative humidities. In this way, it was possible to successfully estimate enzyme retention during drying by means of numerical analysis, solving the nonlinear dehydration equation coupled with the enzymatic inactivation reaction. Yoshii *et al.* (2005) studied the deactivation of alcohol dehydrogenase (ADH) in a drying suspended droplet containing mixed carbohydrates, namely trehalose and randomly methylated β-cyclodextrin (RM-β-CD). They suggested that trehalose was the best excipient and RM-β-CD had a stabilizing effect for alcohol dehydrogenase during drying. Meerdink and van't Riet (1991), and Meerdink (1993) investigated the inactivation of thermo-stable α-amylase in maltodextrin solution droplets, generated by electrostatic atomization and dried during the free fall vertically through a drying tower. The residual activity of thermo-stable

α-amylase during drying was predicted with a first-order Arrhenius-type mathematical model. For this purpose, Meerdink and van't Riet (1991) described the kinetic constant of the deactivation reaction, k_d, as a water-dependent function of the deactivation energy E_d and the pre-exponential factor k_0 as follows:

$$\frac{k_d}{k_{0,\infty}} = \exp\left(cX^d - \frac{E_{d,0} + bX^a}{RT}\right) \tag{6.11}$$

Here, X is the water content on a dry basis. The parameters a, b, c, d, $k_{0,\infty}$ and $E_{d,0}$ were estimated with separate experiments, each of them conducted at constant water content and constant temperature.

6.4.4.2 Stabilization of Enzymes During Spray Drying: Effects of Formulation Composition

Effect of Enzyme Content on the Stabilization of Enzyme Activity in Spray-Dried Powder
The initial enzyme concentration in the feed liquid was found to affect the stability of enzyme activity during spray drying (Yoshii *et al.*, 2008). Trehalose solution of 30 wt% containing alcohol dehydrogenase (ADH) at five different ADH contents was spray-dried at 120 °C inlet air temperature with a rotary disk atomizer. The retention of ADH activity is presented in Fig. 6.33 as a function of the initial amount of ADH in the formulation solution. The retention of ADH increases linearly in the low concentration region of ADH, reaching a plateau value of around 2.8 times higher activity than at lower initial ADH content. ADH molecules appear to mutually protect themselves during spray drying.

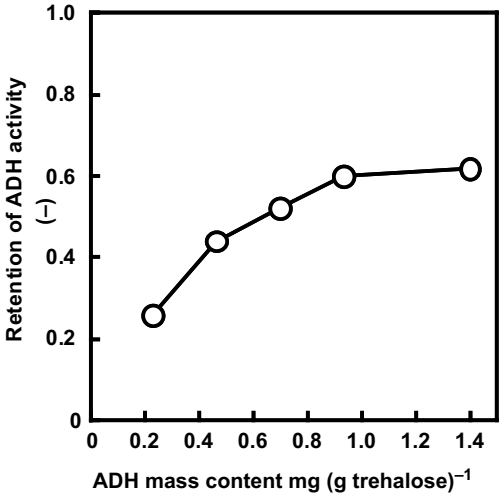

Fig. 6.33 Effect of ADH mass content on the retention of ADH activity. Trehalose mass fraction: 30%; Spray drying conditions: rotary disk atomizer at 30 000 rpm, inlet temperature 120 °C, outlet temperature 70 °C, air mass flow rate 100 kg h^{-1}, liquid feed mass flow rate 40 ml min^{-1}.

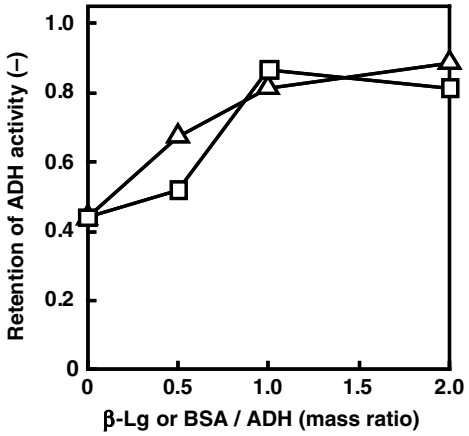

Fig. 6.34 Retention of ADH activity as a function of the mass ratio of additive proteins to ADH for (△) BSA and (□) lactoglobulin. Trehalose mass fraction: 30%, initial amount of ADH: 0.23 mg ADH (g trehalose)$^{-1}$. The spray-drying conditions are the same as in Fig. 6.33.

Enzyme Stabilization by the Addition of Other Proteins and Additives To overcome the thermal damage of ADH during spray drying, Yoshii *et al.* (2008) added a small amount of other proteins such as bovine serum albumin (BSA) or β-lactoglobulin (β-Lg) to the formulation solution. The preservation of ADH activity increased with increasing amount of proteins added, see Fig. 6.34. As mentioned previously, proteins tend to accumulate at the air/droplet interface. Several studies confirmed that the composition of the droplet surface was preserved during spray drying, the protein accumulating on the surface of the spray-dried particle. One of the possible reasons for the protection of ADH by the addition of proteins is that BSA and β-Lg may have covered the surface of the sprayed droplet thus preventing the exposure of ADH to the hot air stream.

Effect of Surfactant and Other Additives on the Retention of Enzyme Activity A common method to improve the preservation of the native structure of an enzyme is to add surfactants to the enzyme solution. Non-ionic surfactants can reduce the aggregation of enzyme proteins during spray drying at or above the critical micelle concentration of the surfactants in the solution (Maa *et al.*, 1997, 1998a; Yoshii *et al.*, 2008). Moreover, increasing the surfactant concentration in a spray solution progressively reduces the inactivation of enzyme during the spray drying. Figure 6.35 illustrates the protective effect of Tween 80 on the inactivation of ADH during spray drying. The addition of 0.047% Tween 80 improved the enzyme activity retention by 9.2%, and the addition of 0.093% by 15.5%. Comparing with BSA and β-Lg, the addition of Tween 80 on ADH has a similar effect.

6.4.4.3 Effect of Process Variables on the Stabilization of Enzymes During Spray Drying

The effect of process conditions on the stability of enzymes during spray drying has been investigated with both a pilot plant spray dryer (Yoshii *et al.*, 2008) and bench-top

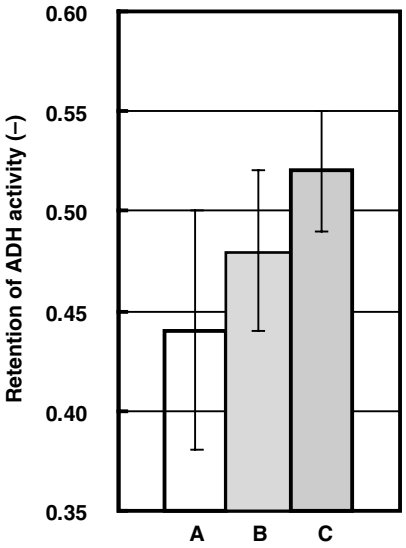

Fig. 6.35 Effect of surfactant (Tween 80) on the retention of ADH activity. A: ADH alone, B: 0.467 mg Tween 80 (g trehalose)$^{-1}$, C: 0.933 mg Tween 80 (g trehalose)$^{-1}$. Trehalose mass fraction: 30%. The spray drying conditions are the same as in Fig. 6.33.

spray dryers (Maa *et al.*, 1998b; Etzel *et al.*, 1996; Meerdink and van't Riet, 1991). The inlet and outlet temperatures of the air are important factors for the preservation of enzymatic activity during drying (Yoshii *et al.*, 2008). The retention of activity at different inlet air temperatures is illustrated in Fig. 6.36 against the outlet air temperature for formulations with and without addition of β-Lg. The outlet air temperature markedly affects the retention of ADH activity, particularly between 70 and 83 °C in the case of the formulation containing β-Lg. At higher outlet temperature, the activity becomes impracticably low and converges to the same value for both formulations, with and without β-Lg. These results infer that it is advisable to keep the outlet air temperature as low as possible, provided that a dried powder can still be produced. Since the inlet and outlet temperature could not be controlled independently in this work, it could not be concluded which temperature was more important in retaining enzymatic activity. Similar results have been obtained experimentally by Etzel *et al.* (1996) for the residual activity of alkaline phosphatase in dependence on the outlet air temperature. The same authors predicted successfully the retention of activity by coupling a mathematical model of droplet drying with a model for the inactivation reaction.

Maa *et al.* (1998b) examined a bench-top spray dryer with the goal of improving the efficiency in both production yield and throughput for the preparation of protein spray-dried powder. They found that a significant loss of particles occurred in the cyclone system. System modifications such as different cyclone designs and replacement of the bag-filter unit by a vacuum system were performed, allowing the protein to be dried at lower inlet/outlet air temperatures.

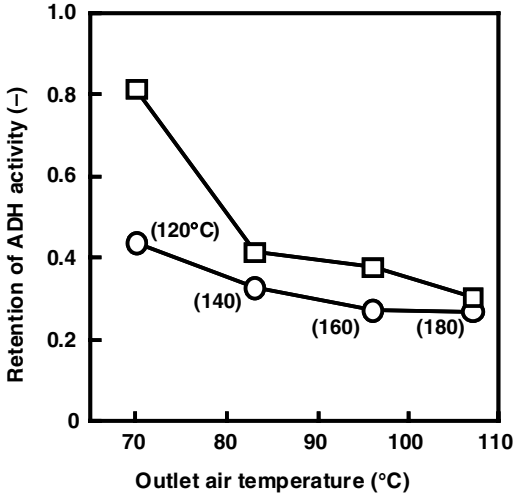

Fig. 6.36 Effect of outlet temperature (abscissa) and inlet air temperature (parameter) on ADH retention during spray drying; ○ ADH alone, □ ADH with β-lactoglobuline. Trehalose mass fraction: 30%, initial ADH content: 0.23 mg ADH (g trehalose)$^{-1}$.

As previously mentioned, the liquid feed undergoes a certain shear stress during the atomization process. To assess the influence of shear stress on enzymatic activity, both a rotary disk atomizer and a two-fluid nozzle were used to spray the liquid feed. As shown in Fig. 6.37, the retention of ADH activity was found to be nearly the same with the examined methods of atomization. These results indicate that the shear

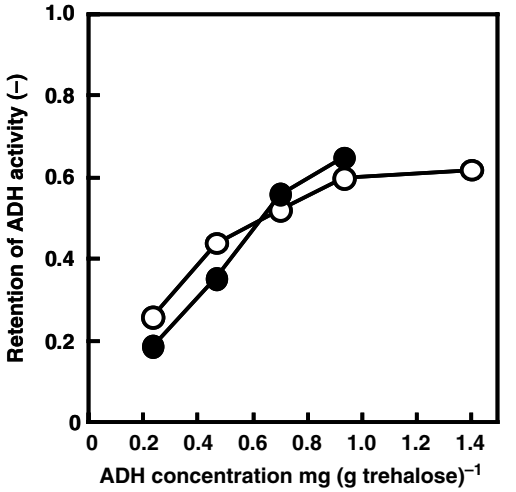

Fig. 6.37 Comparison of the retention of ADH activity between a rotary disk atomizer (○) and a two-fluid nozzle (●); Trehalose mass fraction: 30%. Other conditions are the same as in Fig. 6.33.

stress associated with atomization was either almost equal in both cases or very low for a significant difference to be obtained.

6.4.5 Microencapsulation of Oil

Powdery oils are classified into two categories: formulated microcapsules of oil and encapsulated natural foods. The former are the encapsulated powders of flavors, fish oil and some functional oils such as MCT oil (middle chain triglyceride oil). They are applied to milk, soup and bakery products, because of their beneficial physiological functions. The latter are dehydrated milk powders, dried eggs and powdered soup. The encapsulated oil powder is commonly produced by spray drying of the emulsified oil (O/W emulsion), which is analogous to the technique used for the production of flavor powders. The storage stability of encapsulated oil (avoidance of oxidation of lipids) is extremely important because lipid oxidation leads to loss of nutritional value and undesirable off-flavor formation. It is essential to control the oxidative reaction when highly polyunsaturated fatty acids are involved. Oxidation mechanisms of the bulk oil are well documented, but the oxidation of the encapsulated lipid dispersed in the carbohydrate matrices is fairly complex. Influencing factors for encapsulated lipid oxidation are the type and amount of the wall matrices (carbohydrate and protein), emulsifier, emulsion drop size, storage humidity, and the storage temperature.

6.4.5.1 Spray Drying of Oil Emulsions

The most interesting point concerning microencapsulated oils is the influence of the characteristics of the matrices on encapsulation efficiency, which is defined as the fraction (or percentage) of the encapsulated oil in the total amount of oil (sum of surface oil and encapsulated oil). The amount of surface oil is obtained by simply washing the powder with an organic solvent, such as hexane, prior to extraction. Then, the remaining amount of oil, which is the encapsulated oil, is determined by extraction from the interior of the powdery product.

The amount of lipids washed by hexane from the powder (surface oil) is, therefore, a meaningful indicator for the quality of encapsulation; the smaller the amount of surface oil, the better the encapsulation. Based on this viewpoint, Imagi *et al.* (1990) evaluated the encapsulation ability of wall materials by drying single suspended droplets in equipment of the above-mentioned kind. Both gum arabic and gelatin were confirmed to be excellent wall materials with the highest encapsulation efficiency. However, maltodextrin and pullulane had no emulsifying activity, not being suitable for lipid encapsulation when used alone. Egg albumin and sodium caseinate had a high emulsifying performance, but they also had a poor ability for crust formation on the particle surface, so that the resulting particles were susceptible to oxidation during storage. It can be concluded that it is essential to find an optimal combination of emulsifier and wall material (Matsuno and Adachi, 1993).

Numerous studies have been executed for the microencapsulation of seed oil (flaxseed oil, sea buckthorn seed oil, etc.), fish oil, polyunsaturated fatty acids (PUFAs) and milk fat (Partanen *et al.*, 2008, 2005, 2002; Tuomasjukka *et al.*, 2006; Minemoto *et al.*, 2002a, b; Ishido *et al.*, 2002; Fäldt and Bergenståhl, 1995; Millqvist-Fureby, 2003;

Kim *et al.*, 2002). The cross-sectional structure of the particles from SEM images revealed that small spherical enclosures of oil emulsion appeared in the shell region of the particle. Spray-dried particles were often of hollow structure. The size distribution of the reconstituted emulsion was changed and shifted to larger emulsion droplet sizes, suggesting that partial denaturation of the protein in drying decreases the solubility of proteins (Partanen *et al.*, 2008). The surface composition of the spray-dried particles was studied by ESCA (Partanen *et al.*, 2008; Millqvist-Fureby, 2003; Kim *et al.*, 2002; Fäldt and Bergenståhl, 1995). The oil content near the surface of the particle can be calculated on the basis of the elemental ratio determined by ESCA. The oil/fat coverage on the particle surface depended on the melting temperature of the oil or fat (Fäldt and Bergenståhl, 1995) and the particle size (Partanen *et al.*, 2008).

6.4.5.2 **Oxidation of Lipids Encapsulated in Spray-Dried Particles**

During the last two decades, numerous studies have focused on the impact of the relative humidity of the environmental air on the oxidative stability of encapsulated lipids (Partanen *et al.*, 2008, 2005, 2002; Tuomasjukka *et al.*, 2006; Minemoto *et al.*, 2002a, b; Ishido *et al.*, 2002). An excellent review on the oxidation of micro-encapsulated oils has been recently provided by Velasco *et al.* (2003). In previous sections, the release rate and the oxidation rate of encapsulated flavor were shown to be closely related to the relative humidity – the relationship being very complicated and depending on the glass transition temperature of the wall materials. The effects of relative humidity on the oxidation of oil described in the literature are in agreement with a stability map proposed by Labuza (1971), which suggests a high rate of oxidation at both low and high values of relative humidity (Minemoto *et al.*, 2001; Partanen *et al.*, 2008). This behavior is illustrated in Fig. 6.38. Partanen *et al.* (2008) explained the high rate of oxidation at very dry conditions by cracking of the wall matrix that enhances oxygen diffusion. At high relative humidity, cavities promoting

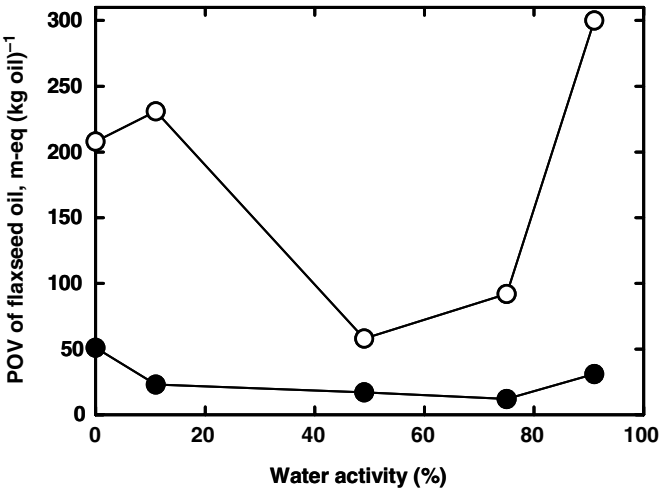

Fig. 6.38 Influence of water activity (relative humidity) on the peroxide value (POV) of bulk flaxseed oil (○) and of flaxseed oil encapsulated in spray-dried WPI (●) after 9 w of storage at 37 °C.

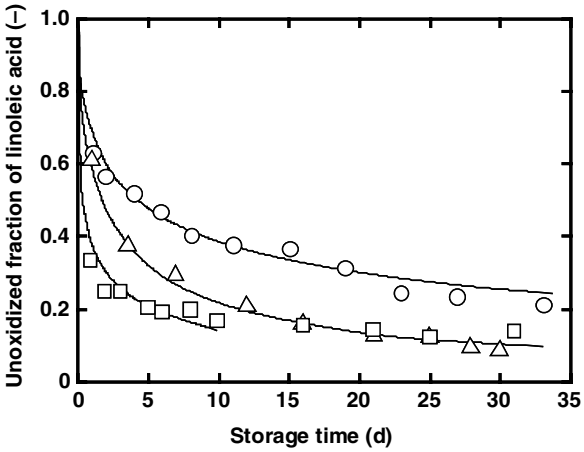

Fig. 6.39 Effect of the emulsion size on the oxidation process of linoleic acid encapsulated in spray-dried powders; Storage at 37 °C and 12% of relative humidity. Emulsion droplet size: ○ 1.04 μm, △ 1.44 μm, □ 2.13 μm.

the oxygen transfer may be formed between aggregations of oil globules. The size of the oil emulsion affects the stability of linoleic acid encapsulated in spray-dried powder (Minemoto *et al.*, 2002a). The smaller the emulsion drop size, the slower the oxidation, as shown in Fig. 6.39, because finer emulsion droplets can more easily be embedded inside dried particles. The oxidation process of linoleic acid encapsulated in spray-dried particles was simulated numerically, based on the assumption that the bulk linoleic acid can be oxidized following the autocatalytic reaction scheme. The oxidation rate constant was related to the free energy of activation according to Eyring's theory. The numerical results correlated well with the experimental oxidation data (Ishido *et al.*, 2002).

6.5
General Quality Aspects

Experimental techniques for the characterization of drying processes and dried products have been presented in great detail in Volume 2 of this series. Additionally, several specific quality aspects of spray-dried powders have been discussed extensively in the foregoing sections of this chapter. This discussion will be concluded by brief reference to some less specific, general quality features of various spray-dried products.

6.5.1
Porosity of Spray-Dried Particles and Species Distribution

The bulk density of a powder, which often is an important product quality aspect, depends, among others, on the inter-particulate porosity. The porosity of particle

layers and the pore size distribution are frequently obtained by mercury porosimetry (Washburn, 1921; Dullien and Batra, 1970). There is a distinct increase in the penetration pressure when the liquid metal enters from inter-particulate voids (void spaces between the spray-dried particles) into the intra-particulate openings (pores within the particles) as these are smaller by usually at least one order of magnitude. Besides this overall assessment of porosity, local examinations and visualizations are also possible by means of X-ray tomography, as shown in Lim and Barigou (2004) and Bröckel *et al.* (2007, Vol. 2). The local composition of individual elements within an agglomerate system is only partly visible in SEM, but can be verified by EDX (energy dispersive X-ray method) and EDXRF (energy dispersive X-Ray fluorescence specroscopy), see for example, van Grieken and Markowicz (2002) and Beckhoff *et al.* (2006).

6.5.2
Strength of Particles and Attrition

The strength and hardness of particles can be obtained by single particle measurement of the yield stress with an indentometer, see for example, McGlinchey (2005), or with a simple pressure test device (Antonyuk, 2009; Grauherr, 1993). The particle strength is of special importance in the ceramics industry, where particles have to be subsequently pressed in molds to form larger and compact specimens which later undergo thermal treatment such as sintering (Bröckel *et al.*, 2007, Vol. 1; Sheng *et al.*, 2004; Samimi *et al.*, 2005; Rahaman, 1995; Salmang and Scholze, 2007). The lower the porosity of the specimen after the compression, the lower the residual porosity after the sintering process (Agniel, 1992). To obtain a dense structure during the compression step, the spray-dried particles must considerably yield and deform at the contact points. A similar situation can be found when tablets of pharmaceutical materials are formed from spray-dried particles (Alderborn and Nyström, 1996; Huntington, 2004; Yaginuma *et al.*, 2007). Also here, a certain compressibility of the spray-dried particles is required, together with a good flowability of the feed powder. The deformation of the feed particles at contact points is necessary in order to obtain tablets with uniform strength and porosity.

Other applications such as spray-dried catalysts require very high strength and abrasion resistance of the particles, even at high temperatures. Spray-dried catalysts have, typically, a particle size in the range 60 to 80 μm, corresponding to their frequent use in fluidized beds or in pneumatic transportation systems designed to serve as reactors. High strength can be achieved by layers of abrasion-resistant additives in the spray-dried slurry, such as silicon dioxide, in molecular or submicron size, that migrates to the shell of the particles during the spray-drying step. However, a certain porosity of the outer layer is also important for the mass transfer of reactants to the active sites within the pore system of the spray-dried particles. At least large pores must be kept open to provide access to deeper layers inside the particles. For the design of catalyst particles see for example, Bröckel *et al.* (2007, Vol. 2), Uihlein (1993), Kastner *et al.* (2001).

Different tests are available to measure the attrition behavior of particles. In the pharmaceutical industry, the friability of powders or granules is tested by tumbling

the particles in a drum and checking for the resulting fines (ISO Tumble Drum Test 3271, 1975 and 1995). An alternative option is to operate an air jet sieve for a given time and air differential pressure, and to determine the loss of fines during that period. Another method applies pneumatic transportation systems and impact plates or cyclones to trigger abrasion in a well-defined manner (Antonyouk, 2006; Pitchumani *et al.*, 2003; Schultz and Kleinebudde, 1995).

6.5.3
Bulk Density and Product Flowability

The bulk density of powders can be measured for example, with the Hosokawa powder characterization tester (www.hmicronpowder.com, McGlinchey (2005)). The flowability of powders can be quantified either in shear cells at considerably low normal pressure (Schwedes and Schulze, 1990) or with small standardized storage bins taking the mass flow over time. The angle of repose, when the sprayed powder leaves a standardized laboratory bin, is also an indicator of the flowability of powders (see e.g., DIN ISO 4490, McGlinchey (2005), Wouters and Geldard (1996)). More recent methods are the agitated cell with fluidization ("Powder Flow Analyzer" by Stable Microsystems: www.stablemicrosystems.com) and the already mentioned versatile powder characterization tester provided by Hosokawa. High flowability is needed to feed the particles into fast-running tableting machines. The dosing system of tableting machines relies fully on the volumetric particle feeding system to obtain uniform tablet masses as superficial feed material is removed from the molds before compression. Even so, additives may help to improve the flowability of the particles (Yaginuma *et al.*, 2007). The bulk density of the particles, therefore, must be maintained within narrow limits. The bulk density can be determined as "poured bulk density," just by pouring the particles from above into a cylinder (DIN EN 725-9, 2006; DIN EN 1236, 1995), or as "tapped density," when this cylinder is tapped several times before measurement (DIN EN 725-8, 2006). To obtain the right volume the surplus particles are best removed by leveling the surface with a straight edge. Sometimes also the "aerated density" is needed for the design of fluidized beds. It may be determined with, for example, the "Powder Flow Analyzer." Spray dried particles with a grain size of 60 to 100 μm lie within the optimal operation range of fluidized beds (McGlinchey, 2005).

6.5.4
Residual Moisture

Usually the residual moisture is obtained by keeping the particles for a given time in a heating chamber at specified air temperature and humidity, and recording the weight loss by removal of volatiles. A faster measurement is obtained with infrared irradiation directly on a drying balance. However, frequently the equilibrium moisture depends on the temperature of the stove and on the air humidity according to a product-specific sorption isotherm. This is true for most organic materials. Moreover, the transition between different crystal hydrate states and crystal water release has to be considered, as they depend on temperature.

In some cases the chemical method given by Karl–Fischer titration can also be applied for residual water determination. This method is based on oxidizing methyl sulfite with iodine into colorless iodide and methyl sulfate. The reaction only takes place when free water is available in the system.

Additional, recently developed methods for the determination of residual water content are the near infrared (NIR) absoption method and nuclear magnetic resonance (NMR). The NMR method has been successfully used for the quick determination of residual water with high spatial and temporal resolution in bulk materials such as granules, applying a magnetic field gradient approach (Blümich, 2005).

6.5.5
Reconstitution Behavior

The reconstitution behavior of porous particles (their so-called "instant properties") can be explained by the fact that the solvent has to penetrate first into the pores of the particles in order to loosen contact forces by, for example, dissolving contact bridges formed by crystals or amorphous material between primary particles (Pfalzer *et al.*, 1973; Schubert, 1975) or by reducing inter-particulate van der Waals forces. The penetration time of the liquid into a porous spray-dried particle with diameter d (wetting time) is given by the well-known Washburn equation (Washburn, 1921; Schubert, 1990):

$$t_{\text{wet}} = \frac{8d^2(1-\varepsilon)\mu}{\varepsilon d_{\text{pr}}\sigma \cos\theta_{\text{eff}}} \tag{6.12}$$

Here, d_{pr} is the Sauter mean diameter of the primary particles originally dispersed in the feed slurry of the spray drier, σ is the surface tension of the liquid, ε is the porosity of the spray dried particle, μ is the viscosity of the penetrating liquid, and θ_{eff} is the mean wetting angle within the pore system. The latter is always larger than the local contact angle θ. One can expect fast penetration and high dissolving velocities when the contact angle is small (good wetting properties). Larger pores lead to faster penetration. However the porosity must not exceed a certain limit, typically $\varepsilon \leq 0.5$, otherwise the capillary transport may be interrupted within the pore system.

The wetting process of powder beds, which as a precondition for the dispersion of the powder particles in a liquid, is, in a similar way as before, determined by the course of liquid penetration into the powdery material. The kinetics of liquid penetration can be measured either by monitoring the weight of the powder layer during wetting or by observing the movement of the liquid front (Teipel, 2005). The liquid front can be more easily observed when the powder layers are prepared with an inclined surface and brought into contact with the liquid from below. The propagation of the wetting boundary is visible in the form of a moving dark-color border and can be documented by photographic means (Wollny and Schubert, 1990). For practical assessment of the reconstitution behavior of spray-dried particles or powders an immersion test has been developed. The particle layer is suddenly

contacted from below with the liquid by removing a sheet at its bottom. The height of the powder layer surface is continuously measured giving information about the simultaneous wetting and sinking behavior of the particles due to capillary effects and gravity (Hogekamp and Pohl, 2004). Re-agglomeration of spray-dried particles often provides improved reconstitution behavior. This can be achieved by use of counter-currently operated spray dryers, as in the detergent industry (Rähse, 2007), with integrated fluidized beds (Herbener, 1987; Masters, 1991) or even with a subsequent external agglomeration step.

The dissolving and dispersing behavior of complexly formulated particles has to be measured in laboratory devices either by optical particle analysis, or by chemical analysis of dissolved matter within the solution or suspension. For that purpose, the spray particles are positioned in baskets within stirred containers, and the light extinction is measured in the suspension or the concentration of dissolved chemical species is recorded versus time (Schubert, 1990; Hogekamp and Pohl, 2004). Similar systems are applied to assess the release functions of pharmaceuticals (Martin and Leuenberger, 2002; Schultz and Kleinebudde, 1997).

6.6 Concluding Remarks

It has been shown that the particle formation and the final shape of particles are strongly related to the materials contained in the liquid feed to the spraying and drying system. Besides the materials introduced as a suspension, solution or as a complex dispersion, the drying conditions, and the preceding drop size dominating the evolving particle size play dominant roles in the formation of the structure and in providing a high final biochemical or chemical product quality. This is obvious, when drying complex molecules such as proteins, or when high retention is desired, when drying flavors. Protective agents may help in maintaining the high quality of the product by protecting the structure of sensitive species. However, the temperature of the drying air often also has to be kept within limits in order to avoid unwanted oxidation despite increased heat losses. The spraying process as well as the flow within industrial drying towers is usually subject to stochastic fluctuations, mainly caused by turbulence. This leads to non-uniform trajectories and drying histories of individual particles with different sizes and may also cause agglomeration. It will be an incentive in future to overcome unwanted fluctuations as well as to provide sprays with narrow drop size distribution as a prerequisite for high quality uniform products with largely identical particle morphologies.

Additional Notation Used in Chapter 6

B_M	Spalding transfer number	–
C	concentration	kg m^{-3}
E	Young's modulus	N m^{-2}

G	free energy	J kg^{-1}
k	Boltzmann constant	J K^{-1}
k_d	deactivation rate constant	s^{-1}
k_R	release rate	various
k_x	oxidation rate constant	s^{-1}
k_1	relaxation rate constant	s^{-1}
R	retention	–
T_g	glass transition temperature	°C

Greek Letters

ζ	zeta potential	V
ν	Poisson's ratio	–
τ	relaxation time	s

Subscripts

B	buckling
d	droplet
d	deactivation
pr	primary particle
S	surface
shell	shell
sp	suspension particle

Abbreviations

ADH	alcohol dehydrogenase
BSA	bovine serum albumin
CD	cyclodextrin
CFD	computational fluid dynamics
CLSM	confocal laser scanning microscopy
CMC	carboxymethylcellulose
CRP	constant rate period
DE	dextrose equivalent
DHA	docosahexaenoic acid
EDX	energy dispersive X-ray spectroscopy
EDXRF	energy dispersive X-ray fluorescence spectroscopy
EPA	eicosapentaenoic acid
ESCA	electron spectroscopy for chemical analysis
FCC	fluid catalytic cracking
FT-IR	Fourier transform infrared spectroscopy
GA	gum Arabic
KWW	Kohlrausch–Williams–Watts

Lg	lactoglobulin
MCT	middle chain triglyceride
MD	maltodextrin
NIR	near-infrared
NMR	nuclear magnetic resonance
O/W	oil in water
POV	peroxide value
PTR-MS	proton transfer reaction mass spectrometry
PUFA	polyunsaturated fatty acid
RH	relative humidity
RM	randomly methylated
rhGH	human growth hormone
SBS	styrene-butadiene-styrene
SE-HPLC	size-exclusion high-performance liquid chromatography
SEM	scanning electron microscopy
SSPS	soluble soybean polysaccharide
VPO	vanadium phosphate oxide
WLF	William–Landel–Ferry
WPI	whey protein isolate

References

Abramzon, B., Sirignano, W. A., 1989. Droplet vaporization model for spray combustion calculations. *Int. J. Heat Mass Transfer* **32**: 1605–1618.

Adhikari, B., Howes, T., Bhandari, B. R., Troung, V., 2003. Surface stickiness of drops of carbohydrate and organic acid solutions during convective drying: Experiments and modeling. *Drying Technol.* **21**(5): 839–873.

Adhikari, B., Howes, T., Leocomte, D., Bhandari, B. R., 2005. A glass transition temperature approach for the prediction of the surface stickiness of a drying droplet during spray drying. *Powder Technol.* **149**: 168–179.

Adler, M., Lee, G., 1999. Stability and surface activity of lactate dehydrogenase in spray-dried trehalose. *J. Pharm. Sci.* **88**: 199–208.

Agniel, Y., 1992. Bedeutung der Einzelgranalieneigenschaften zur Defektvermeidung in trockengepressten keramischen Modellpulvern. Diss., TH Karlsruhe, Germany.

Alamilla-Beltrán, L., Chanona-Pérez, J. J., Jiménez-Aparicio, A. R., Gutiérrez-López, G. F., 2005. Description of morphological changes of particles along spray drying. *J. Food. Eng.* **67**: 179–184.

Alderborn, G., Nyström C., 1996. *Pharmaceutical powder compaction*. Marcel Dekker, New York, USA.

Anandaraman, S., Reineccius, G. A., 1986. Stability of encapsulated orange peel oil. *Food Technol.* **40**(11): 88–94.

Anese, M., Manzocco, L., Maltini, E., 2005. Effect of coffee physical structure on volatile release. *Eur. Food Res. Technol.* **221**: 434–438.

Ansari, A., Jones, C. M., Henry, E. R., Hofrichter, J., Eaton, W. A., 1992. The role of solvent viscosity in the dynamics of protein conformational-changes. *Science* **256**(5065): 1796–1798.

Antonyouk, S., 2006. Deformations- und Bruchverhalten von kugelförmigen Granulaten bei Druck- und Stossbeanspruchung. Diss., Universität Magdeburg, Germany.

Antonyuk, S., Heinrich, S., van Buijtenen, M., Deen, N. G., Kuipers, J., 2009. Feuchteeinfluss auf das Partikelstoßverhatten in Wirbelschichten. *Chem Ing. Tech.* **81**: 1177– 1178.

Barbosa-Cánovas, G. V., Ortega-Rivas, E., Juliano, P., Yan, H., 2005. *Food powders: physical properties, processing, and functionality.* Springer, New York, USA, pp. 199–220.

Beckhoff, B., Kannengiesser, B., Langhoff, N., Wedell, R., Wolff, H., 2006. *Handbook of practical X-ray fluorescence analysis.* Springer, Berlin, Germany.

Belton, P. S., Gill, A. M., 1994. IR and Raman spectroscopic studies of the inter-action of trehalose with hen egg white lysozyme. *Biopolymers* **34**: 957–961.

Beristain, C. I., Azuara, E., Vernon-Carter, E. J., 2002. Effect of water activity on the stability to oxidation of spray-dried encapsulated orange peel oil using mesquite gum (Prosopis Juliflora) as wall material. *J. Food Sci.* **67**: 206–211.

Bhandari, B. R., Dumoulin, E. D., Richard, H. M. J., Noleau, I., Lebert, A. M., 1992. Flavor encapsulation by spray drying: Application to citral and linalyl acetate. *J. Food Sci.* **57**(1): 217–221.

Bhandari, B. R., Howes, T., 1999. Implication of glass transition for the drying and stability of dried foods. *J. Food Eng.* **40**: 71–79.

Bird, R. B., Steward, W. E., Lightfoot, E. N., 2002. *Transport phenomena*. 2nd edn, John Wiley & Sons, New York, USA.

Blümich, B., 2005. *Essential NMR for scientists and engineers.* Springer, Berlin, Germany.

Bomben, J. L., Bruin, S., Thijssen, H. A. C., Merson, R. L., 1973. Aroma recovery and retention in concentration and drying of foods, in *Advances in Food Research* (eds G. S. Stewart, E. M. Mrak, C. O. Chichester). Academic Press, New York, USA, Vol. 20: pp. 1–111.

Brenn, G., Wiedemann, T., Rensink, D., Kastner, O., Yarin, A. L., 2001. Modeling and experimental investigation of the morphology of spray dried particles. *Chem. Eng. Technol.* **24**(11): 1113–1116.

Broadhead, J., Rouan, S. K. E., Rhodes, C. T., 1992. The spray drying of pharmaceuticals. *Drug Dev. Ind. Pharm.* **18**: 1169–1206.

Bröckel, U., Meier, W., Wagner, G., 2007. *Product Design and Engineering.* Vol. 1 and 2, Wiley-VCH. Weinheim, Germany.

Carpenter, J., Crowe, J. H., 1984. An infrared spectroscopy study of the interactions of carbohydrates with dried proteins. *Biochemistry* **28**: 3916–3922.

Chang, Y. I., Scire, J., Jacobs, B., 1988. Effect of particle size and microstructure properties on encapsulated orange oil, in *Flavor encapsulation* (eds S. J. Risch, G. A. Reineccius). American Chemical Society, Washington DC, USA, pp. 87–102.

Constantino, H. R., Firouzabadian, L., Wu, C., Carrasquillo, K. G., Griebenow, K., Zale, S. E., Tracy, M. A., 2001. Protein spray freeze drying, Part 2: Effect of formulation variables on particle size and stability. *J. Pharm. Sci.* **91**: 388–395.

Contractor, R. M., Bergna, H. E., Horowitz, H. S., Blackstone, C. M., 1987. Butane oxidation over vanadium phosphate catalysts. *Catal. Today* **1**: 49–58.

Coumans, W. J., Kerkhof, P., Bruin, S., 1994. Theoretical and practical aspects of aroma retention in spray drying and freeze drying. *Drying Technol.* **12**: 99–149.

Crowe, J. H., Crowe, L. M., Chapman, D., 1984. Preservation of membranes in anhydrobiotic organisms: The role of trehalose. *Science* **223** (4637): 701–703.

Dicoi, O., Walzel, P., 1998. Vergleich verschiedener Modellansätze zur Tropfenverdunstung von Einzeltropfen. *Proceedings of Spray '98*, Essen, Germany.

DIN EN 735-8, 2006. Bestimmung der geklopften Schüttdichte.

DIN EN 725-9, 2006. Bestimmung der Schüttdichte.

DIN EN 1236, 1995. Bestimmung der Schüttdichte.

DIN ISO 4490, Ermittlung des Fließverhaltens mit Hilfe eines kalibrierten Trichters.

Dronen, D. M., Reineccius, G. A., 2003. Rapid analysis of volatile release from powders using dynamic vapour sorption atmospheric pressure chemical ionization

mass spectrometry. *J. Food Sci.* **68**: 2158–2162.
Dullien, F. A. L., Batra, V. K., 1970. Determination of the structure of porous media. *Ind. Eng. Chem.* **62**(10): 25–53.
Eggers, J., Villermaux, E., 2008. Physics of liquid jets. *Rep. Progr. Phys.* **71**: 1–79.
El-Sayed, T. M., Wallack, D. A., King, C. J., 1990. Changes in particle morphology during drying of drops, Part 1: Effects of composition and drying conditions. *Ind. Eng. Chem. Res.* **29**: 2346–2354.
Etzel, M. R., Shen, S.-Y., Halverson, S. L., Budijono, S., 1996. Enzyme inactivation in a droplet forming a bubble during drying. *J. Food Eng.* **27**: 17–34.
Fäldt, P., Bergenståhl, B., 1995. Fat encapsulation in spray-dried food powders. *J. Am. Oil Chem. Soc.* **72**: 171–176.
Finney, J., Buffo, R., Erinaceous, G. A., 2002. Effect of type of atomization and processing temperatures on the physical properties and stability of spray-dried flavors. *J. Food Sci.* **67** (3): 1108–1114.
Flory, P. J., 1942. Thermodynamics of high polymer solutions. *J. Chem. Phys.* **10**(51): 51–61.
Franks, F., Hately, R. H. M., Mathias, S. F., 1994. Material science and the production of shelf-stable biologicals. *Bio. Pharm.* **4**: 253–256.
Fries, M., 2008. Produktgestaltung keramischer Sprühgranulate für die uniaxiale Pressverdichtung zu großformatigen Bauteilen. Diss., TU Bergakademie Freiberg, Germany.
Furuta, T., Tsujimoto, S., Okazaki, M., Toei, R., 1984. Effect of drying on retention of ethanol in maltodextrin solution during drying of a single droplet. *Drying Technol.* **2**: 311–327.
Furuta, T., Hayashi, H., Ohashi, T., 1994. Some criteria of spray dryer design for food liquid. *Drying Technol.* **12**: 151–177.
Gacular, M. C., Jr., Kubala, J. J., 1975. Statistical models for shelf life failures. *J. Food Sci.* **40**: 404–409.
Garmise, R. J., 2007. Novel dry powder preparations of whole inactivated influenza virus for nasal vaccination. *APS Pharm. Sci. Tech.* **8**(4): Article 81, E1–E9.
Gibbs, B. F., Kermasha, S., Alli, I., Mulligan, C. N., 1999. Encapsulation in the food industry: A review. *Int. J. Food Sci. Nutr.* **50**: 213–224.
Giunchedi, P., Conte, U., 1995. Spray-drying as a preparation method of micro-particulate drug delivery systems: An overview. *STP Pharma Sci.* **5**: 276–290.
Gnielinski, V., Mersmann, A., Thurner, F., 1993. *Verdampfung, Kristallisation, Trocknung*. Vieweg Verlag, Braunschweig, Germany.
Gordon, M., Taylor, J. S., 1952. Ideal copolymers and the second-order transitions of synthetic rubbers, Part 1: Non-crystalline copolymers. *J. Appl. Chem.* **2**: 493–500.
Grauherr, B., 1993. Herstellung und Charakterisierung keramischer Wirbelschichtgranulate und ihr Einfluss auf das Gefüge und die Eigenschaften plasmagespritzter Schichten. Diss., RWTH Aachen, Germany.
Greenwald, G. C., 1980. Particle morphology in the spray drying of foods. Diss., University of California, Berkeley, USA.
Greenwald, G. C., King, C. J., 1981. The effects of design and operating conditions on particle morphology for spray-dried foods. *J. Food Process Eng.* **4**: 171–187.
Greenwald, G. C., King, C. J., 1982. The mechanism of particle expansion in spray drying of foods. *AICHE Symp. Ser. Food Process Engineering* **78**(218): 101–110.
Groenewold, C., Möser, C., Groenewold, H., Tsotsas, E., 2002. Determination of single particle drying kinetics in an acoustic levitator. *Chem. Eng. J.* **86**: 217–222.
Gunning, Y. M., Gunning, P. A., Kemsley, E. K., Parker, R., Ring, S. G., Wilson, R. H., Blake, A., 1999. Factors affecting the release of flavor encapsulated in carbohydrate matrixes. *J. Agric. Food Chem.* **47**: 5198–5205.
Hadinoto, K., Kewu, Z., Tan, R. B. H., 2007. Drug release study of large hollow nanoparticulate aggregates carrier particles for pulmonary delivery. *Int. J. Pharm.* **341** (1–2): 195–206.
Hecht, H. P., King, C. J., 2000a. Spray drying: Influence of developing drop morpholog on drying rates and retention of volatile substances, Part 1: Single drop experiments. *Ind. Eng. Chem. Res.* **39**: 1756–1765.

Hecht, J. P., King, C. J., 2000b. Spray drying: Influence of developing drop morphology on drying rates and retention of volatile substances, Part 2: Modeling. *Ind. Eng. Chem. Res.* **39**: 1766–1774.

Heldmann, D. R., 1974. An analysis of atmospheric freeze drying. *J. Food Sci.* **39**: 147–155.

Herbener, R., 1987. Staubarme Pulver durch Sprühtrocknen – Erfahrungen mit neueren Techniken. *Chem.-Ing.-Tech.* **59**: 112–117.

Hogekamp, S., Pohl, M., 2004. Methoden zur Beurteilung des Befeuchtungs- und Dispergierverhaltens von Pulven. *Chem.-Ing.-Tech.* **76**: 385–390.

Huntington, D. H., 2004. The influence of the spray drying process on product properties. *Drying Technol.* **22**: 1261–1288.

Imagi, J., Kako, N., Nakanishi, K., Matsuno, R., 1990. Entrapment of liquid lipids in matrices of saccharides. *J. Food Eng.* **12**: 207–222.

Ishido, E., Hakamata, K., Minemoto, Y., Adachi, S., Matsuno, R., 2002. Oxidation process of linoleic acid encapsulated with a polysaccharide by spray-drying. *Food Sci. Technol. Res.* **8**(1): 85–88.

Ishido, E., Minemoto, Y., Adachi, S., Matsuno, R., 2003. Heterogeneity during autoxidation of linoleic acid encapsulated with a polysaccharide. *J. Food Eng.* **59**: 237–243.

Jørgensen, K., 2005. Drying rate and morphology of slurry droplets. Diss., Technical University of Denmark, Lyngby, Denmark.

Karel, M., Langer, R., 1988. Controlled release of food additives, in *Flavor encapsulation* (eds S. J. Risch, G. A. Reineccius). American Chemical Society, Washington DC, USA, pp. 67–77.

Kastner, O., Rensink, G., Brenn, G., Tropea, C., 2001. The acoustic tube levitator – a novel device for determining the drying kinetics of single droplets. *Chem. Eng. Technol.* **24**: 335–339.

Kawamura, Y., Nakanishi, K., Matsuno, R., Kamikubo, T., 1981. Stability of immobilized α-chymotrypsin. *Biotechnol. Bioeng.* **23**: 1219–1236.

Kilburn, D., Claude, J., Schweizer, T., Alam, A., Ubbink, J., 2005. Carbohydrate polymers in amorphous states: An integrated thermodynamic and nanostructural investigation. *Biomacromolecules* **6**: 864–879.

Kim, Y. D., Morr, C. V., 1996. Microencapsulation properties of gum arabic and several food proteins: Spray-dried orange oil emulsion particles. *J. Agric. Food Chem.* **44**: 1314–1320.

Kim, E. H.-J., Chen, X. D., Pearce, D., 2002. Surface characterization for four industrial spray-dried dairy powders in relation to chemical composition, structure and wetting property. *Colloids Surf. B* **26**: 197–212.

King, C. J., 1995a. Spray drying: Retention of volatile compounds revisited. *Drying Technol.* **13**: 1221–1240.

King, A. H., 1995b. Encapsulation of food ingredients: A review of available technology, focusing on hydrocolloids, in *Encapsulation and controlled release of food ingredients* (eds S. J. Risch, G. A. Reineccius). American Chemical Society, Washington DC, USA, pp. 26–39.

Koch, M., Walzel, P., 2001. Migration of solutes in drying suspension droplets. *Proceedings of the Conference on Spray Drying and Related Processes*, Dortmund, Shaker Verlag, Aachen, Germany.

Lamprecht, A., Schafer, U. F., Lehr, C. M., 2000a. Characterization of microcapsules by confocal laser scanning microscopy: Structure, capsule wall composition and encapsulation rate. *Eur. J. Pharm. Biopharm.* **49**: 1–9.

Lamprecht, A., Schafer, U. F., Lehr, C. M., 2000b. Structural analysis of microparticles by confocal laser scanning microscopy. *AAPS Pharm. Sci. Tech.* **1**(3): 10–19.

Lamprecht, A., Schafer, U. F., Lehr, C. M., 2000c. Visualization and quantification of polymer distribution in microcapsules by confocal laser scanning microscopy (CLSM). *Int. J. Pharm.* **196**: 223–226.

Landström, K., Alsins, J., Bergenståhl, B., 2000. Competitive protein adsorption between bovine serum albumin and β-lactoglobulin during spray-drying. *Food Hydrocolloids* **14**(1): 75–82.

Labuza, T., 1971. Kinetics of lipid oxidation in foods. *CRC Rev. Food Technol.* **2**: 335–405.

Labrousse, S., Roos, Y., Karel, M., 1992. Collapse and crystallization in amorphous matrices with encapsulated compounds. *Sci. Aliment.* **12**: 757–769.

Leahy, M. M., Anandaraman, S., Bangs, W. E., Reineccius, G. A., 1983. Spray drying of food flavors, Part 2: A comparison of encapsulating agents for the drying of artificial flavors. *Perfum. Flavorist* **8**: 49.52.

Lee, G., 2002. Spray drying of proteins, in *Rational design of stable protein formulations* (eds J. F. Caprenter, M. C. Manning). Plenum Press, New York, USA, pp. 135–158.

Levine, H., Slade, L., 1986. A polymer physico-chemical approach to the study of commercial starch hydrolysis products (SHPs). *Carbohydr. Polym.* **6**: 213–244.

Levi, G., Karel, M., 1995. The effect of phase transitions on release of n-propanol entrapped in carbohydrate glasses. *J. Food Eng.* **24**: 1–13.

Lim, K. S., Barigou, M., 2004. X-ray tomography of cellular food products. *Food Research Int.* **37**(10): 1001–1012.

Liou, J. K., 1982. An approximate method for nonlinear diffusion applied to enzyme inactivation during drying. Diss., Agricultural University Wageningen, The Netherlands.

Liu, X. D., Atarashi, T., Furuta, T., Yoshii, H., Ohkawara, S., 2001. Microencapsulation of emulsified hydrophobic flavors by spray drying. *Drying Technol.* **19**: 1361–1374.

Lohner, H., Czisch, C., Schreckenberg, P., Fritsching, U., Bauckhage, K., 2005. Atomization of viscous melts. *Atomization Spray* **15**(2): 169–180.

Maa, Y.-F., Hsu, C. C., 1996. Effect of high shear on proteins. *Biotech. Bioeng.* **51**: 458–465.

Maa, Y.-F., Costantino, H. R., Nguyen, P.-A., Hsu, C. C., 1997. The effect of operation and formulation variables on the morphology of spray-dried protein particles. *Pharm. Dev. Tech.* **2**: 213–223.

Maa, Y.-F., Hsu, C. C., 1997. Protein denaturation by combined effect of shear and air-liquid interface. *Biotech. Bioeng.* **54**: 503–512.

Maa, Y.-F., Nguyen, P.-A., Hsu, S. W., 1998a. Spray-drying of air-liquid interface sensitive recombinant human growth hormone. *J. Pharm. Sci.* **87**: 152–159.

Maa, Y.-F., Nguyen, P.-A., Sit, K., Hsu, S. W., 1998b. Spray-drying performance of a bench-top spray dryer for protein aerosol powder preparation. *Biotech. Bioeng.* **60**: 503–512.

Maas, H. G., Schaldach, G., Walzel, P., Urbanetz, N. A., 2009. Manufacturing of tailor made carrier particles for inhalation therapy by spray drying. *Proceedings of the 11th Intern. Conference on Liquid Atomization and Spray Systems (ICLASS)*, Vail Colorado, USA.

Martin, A. N., Leuenberger, H., 2002. *Physikalische Pharmazie*. 4th edn, Wissenschaftliche Verlagsges., Stuttgart, Germany.

Masters, K., 1991. *Spray drying handbook*. 5th edn, Longman, Burnt Mills/Essex, UK.

Mateus, M.-L., Lindinger, C., Gumy, J.-C., Liardon, R., 2007. Release kinetics of volatile organic compounds from roasted and ground coffee: Online measurements by PTR-MS and mathematical modelling. *J. Agric. Food Chem.* **55**: 10117–10128.

Matsuno, R., Adachi, S., 1993. Lipid encapsulation technology – techniques and applications to food. *Trends Food Sci. Technol.* **4**: 256–261.

McGlinchey, D., 2005. *The characterization of bulk solids*. Blackwell Publishing, Oxford, UK.

McNamee, B. F., O'Riordan, E. D., O'Sullivan, M., 1998. Emulsification and microencapsulation properties of gum arabic. *J. Agric. Food Chem.* **46**: 4551–4555.

McNamee, B. F., O'Riordan, E. D., O'Sullivan, M., 2001. Effect of partial replacemnet of gum arabic with carbohydrates on its microencapsulation properties. *J. Agric. Food Chem.* **49**: 3385–3388.

Meerdink, G., van't Riet, K., 1991. Inactivation of a thermostable-amylase during drying. *J. Food Eng.* **14**: 83–102.

Meerdink, G., 1993. Drying of liquid food droplets: Enzyme inactivation and multi-component diffusion. Diss., Agricultural University Wageningen, The Netherlands.

Menting, L. C., Hoogstad, B., 1967. Volatiles retention during the drying of aqueous

carbohydrate solutions. *J. Food Sci.* **32**: 87–90.

Menting, L. C., Hoogstad, B., Thijssen, H. A. C., 1970. Diffusion coefficients of water and organic volatiles in carbohydrate-water systems. *J. Food Technol.* **5**: 111–126.

Millqvist-Fureby, A., 2003. Characterisation of spray-dried emulsions with mixed fat phases. *Colloids Surf. B* **31**, 65–79.

Minemoto, Y., Adachi, S., Matsuno, R., 2001. Effect of relative humidity during storage on the autoxidation of linoleic acid encapsulated with a polysaccharide by hot-air-drying and freeze-drying. *Food Sci. Technol. Res.* **7**: 91–93.

Minemoto, Y., Hakamata, K., Adachi, S., Matsuno, R., 2002a. Oxidation of linoleic acid encapsulated with gum arabic or maltodextrin by spray-drying. *J. Microencapsulation* **19**: 181–189.

Minemoto, Y., Fang, X., Hakamata, K., Watanabe, Y., Adachi, S., Kometani, T., Matsuno, R., 2002b. Oxidation of linoleic acid encapsulated with soluble soybean polysaccharide by spray-drying. *Biosci. Biotechnol. Biochem.* **66**: 1829–1834.

Minoshima, H., Matsushima, K., Liang, H., Shinohara, K., 2001. Basic model of spray drying granulation. *J. Chem. Eng. Japan.* **34** (4): 472–478.

Minoshima, H., Matsushima, K., Liang, H., Shinohara, K., 2002. Estimation of diameter of granule prepared by spray drying with fast and easy evaporation. *J. Chem. Eng. Japan* **35**: 880–885.

Monse, K., Linnepe, T., Groom, S., Walzel, P., 2001. Influence of nozzle type on particle formation in spray drying. *Proceedings of the Conference on Spray Drying and Related Processes,* Dortmund, Shaker Verlag, Aachen, Germany.

Monse, K., Koch, M., Walzel, P., 2006. Migration der kontinuierlichen Phase beim Trocknen von Suspensionstropfen in einer Trocknungskammer. *Chem.-Ing.-Tech.* **78**: 78–82.

Moreau, D. L., Rosenberg, M., 1993. Microstructure and fat extractability in microcapsules based on whey proteins or mixtures of whey proteins and lactose. *Food Struct.* **12**: 457–468.

Mumenthaler, M., 2000. Atmospheric spray-freeze drying: A suitable alternative in freeze-drying technology. *Int. J. Pharm.* **72**: 97–110.

Nebelung, M., Fries, M., Kraft, T., 2008. Produktdesign von Pressgranulaten – Anforderungen und Realität, in *Pulvermetallurgie: Neue Anforderungen, neue Produkte, neue Verfahren* (ed. H. Kolaska). Heimdall Verlag, Witten, Germany, pp. 107–118.

Nelson, K. A., Labuza, T. P., 1992. Relationship between water and lipid oxidation rates, in *Water activity and glass transition theory* (ed. A. J. St. Angelo). American Chemical Society, Washington DC, pp. 93–103.

Onwulata, C. I., Smith, P. W., Cooke, P. H., Holsinger, V. H., 1996. Particle structures of encapsulated milk fat powders. *Lebebsm.-Wiss. u. Technol.* **29**: 163–172.

Palzer, S., 2005. The effect of glass transition on the desired and undesired agglomeration of amorphous food powders. *Chem. Eng. Sci.* **60**: 3959–3968.

Partanen, R., Raula, J., Seppänen, R., Buchert, J., Kauppinene, E., Forssell, P., 2008. Effect of relative humidity on oxidation of flaxseed oil in spray dried whey protein emulsions. *J. Agric. Food Chem.* **56**: 5717–5722.

Partanen, R., Hakala, P., Siövall, O., Kallio, H., Forssell, P., 2005. Effect of relative humidity on the oxidative stability of microencapsulated sea buckthorn seed oil. *J. Food Sci.* **70**: E37–E43.

Partanen, R., Ahro, M., Hakala, M., Kallio, H., Forssell, P., 2002. Microencapsulation of caraway extract in β-cyclodextrin and modified starches. *Eur. Food Res. Technol.* **214**: 242–247.

Pfalzer, L., Bartusch, W., Heiss, R., 1973. Untersuchungen über die physikalischen Eigenschaften agglomerierter Pulver. *Chem.-Ing.-Tech.* **45**(8): 510–516.

Pitchumani, R., Meesters, G. M. H., Scarlett, B., 2003. Breakage behavior of enzyme granules in a repeated impact test. *Powder Technol.* **130**: 138–146.

Rahaman, M. N., 1995. *Ceramic processing and sintering.* Marcel Dekker, New York, USA.

Rähse, W., 2007. *Produktdesign in der chemischen Industrie.* Springer, Berlin, Germany.

Reineccius, G. A., Coulter S. T., 1969. Flavor retention during drying. *J. Dairy Sci.* **52**(8): 1219–1223.

Reineccius, G. A., Bangs, W. E., 1985. Spray drying of food flavors, Part 3: Optimum infeed concentrations for the retention of artificial flavors. *Perfum. Flavorist* **10**: 27–29.

Reineccius, G. A., 1988. Spray-drying of food flavors, in *Flavor encapsulation* (eds S. J. Risch, G. A. Reineccius). American Chemical Society, Washington DC, USA, pp. 55–66.

Reineccius, G. A., 2005. *Flavor chemistry and technology*. 2nd edn, CRC Press, New York, USA, pp. 351–384.

Ré, M. I., Liu, Y. J., 1996. Microencapsulation by spray drying: Influence of wall systems on the retention of the volatiles compounds. *Proceedings of the 10th International Drying Symposium*, Kraków, 541–549.

Ré, M. I., 1998. Microencapsulation by spray drying. *Drying Technol.* **16**: 1195–1236.

Ré, M. I., 2006. Formulating drug delivery systems by spray drying. *Drying Technol.* **24**: 433–446.

Risch, S. J., 1995. Encapsulation: Overview of uses and techniques, in *Encapsulation and controlled release of food ingredients* (eds S. J. Risch, G. A. Reineccius). American Chemical Society, Washington DC, USA, pp. 2–7.

Risch, S. J., Reineccius, G. A., 1988. Spray-dried orange oil: Effect of emulsion size on flavor retention and shelf stability, in *Flavor encapsulation* (eds S. J. Risch, G. A. Reineccius). American Chemical Society, Washington DC, USA, pp. 67–77.

Roos, Y., 1995. Phase transitions in foods, in *Food science and technology – International series* (No. 360), Academic Press, San Diego/California, USA.

Roos, Y., 2003. Phase and state transitions in food dehydration. *Proceedings of the Symposium EUDrying 03*, Crete, 153–168.

Rosenberg, M., Kopelman, I. J., Talmon, Y., 1985. A scanning electron microscopy study of microencapsulation. *J. Food Sci.* **50**: 139–144.

Rosenberg, M., Kopelman, I. J., Talmon, Y., 1990. Factors affecting retention in spray-drying microencapsulation of volatile materials. *J. Agric. Food Chem.* **38**: 1288–1294.

Rulkens, W. H., Thijssen, H. A. C., 1972. The retention of organic volatiles in spray-drying aqueous carbohydrate solutions. *J. Food Technol.* **7**(1): 95–105.

Rumpf, H., 1975. *Mechanische Verfahrenstechnik*. Carl Hanser Verlag, München, Germany.

Salmang, H., Scholze, H., 2007. *Keramische Verfahrenstechnik*. 7th edn, Springer, Berlin, Germany.

Samimi, A., Hassanpour, A., Ghodiri, M., 2005. Single bulk compression of soft granules: Experimental study and DEM evaluation. *Chem. Eng. Sci.* **60** (14): 3993–4004.

Sankarikutty, B., Sreekumar, M. M., Narayanan, C. S., Mathew, A. G., 1988. Studies on encapsulation of cardamon oil by spray-drying technique. *J. Food Sci. Technol.* **25**: 325–355.

Schubert, H., 1975. Über Grenzflächenvorgänge in der Agglomerationstechnik. *Chem.-Ing.-Tech.* **47**(3): 86.

Schubert, H., 1990. Instantisieren pulverförmiger Lebensmittel. *Chem.-Ing.-Tech.* **62**(11): 892–906.

Schultz, P., Kleinebudde, P., 1995. Determination of pellet friability by use of an air stream apparatus. *Pharm. Ind.* **57**: 323–328.

Schultz, P., Kleinebudde, P., 1997. A new multiparticulate delayed release system, Part 1: Dissolution properties and release mechanism. *J. Contr. Rel.* **47**: 181–189.

Schwedes, J., Schulze, D., 1990. Measurement of flow properties of bulk solids. *Powder Technol.* **61**: 59–68.

Sheng, Y., Briscoe, B. J., Maung, R., Rovea, M. J., 2004. Compression of polymer bound alumina agglomerates at the micro deformation scale. *Powder Technol.* **140**: 228–239.

Shinoda, K., 1978. *Principles of solution and solubility*. Marcel Dekker, New York, USA.

Sirignano, W. A., 1999. *Fluid dynamics and transport of droplets and sprays*. Cambridge University Press, Cambridge, UK.

Sivetz, M., Foote, H. E., 1963. *Coffee processing technology*. AVI Publishing Co., Westport/Connecticut, USA.

Shahidi, F., Han, X. Q., 1993. Encapsulation of food ingredients. *Crit. Rev. Food Sci. Nutr.* **33**(6): 501–547.

Soottitantawat, A., Yoshii, H., Furuta, T., Ohgawara, M., Forssell, P., Partanen, R., Poutanen, K., Linko, P., 2004a. Effect of

water activity on the release characteristics and oxidative stability of d-limonene encapsulated by spray drying. *J. Agric. Food Chem.* **52**: 1269–1276.

Soottitantawat, A., Peigney, J., Uekaji, Y., Yoshii, H., Furuta, T., Ohkawara, M., Linko, P., 2004b. Structural analysis of spray-dried powders by confocal laser scanning microscopy. *Proceedings of the Annual Meeting of IFT 2004*, Las Vegas, 17-G-22.

Soottitantawat, A., Yoshii, H., Furuta, T., Ohgawara, M., Linko, P., 2003. Microencapsulation by spray drying: Influence of emulsion size on the retention of volatile compounds. *J. Food Sci.* **68**: 2256–2262.

Soottitantawat, A., 2005. Influence of emulsion size and powder morphology on the microencapsulation and stability of spray-dried flavors. Diss., Tottori University, Japan.

Soottitantawat, A., Peigney, J., Uekaji, U., Yoshii, H., Furuta, T., Ohgawara, M., Linko, P., 2007. Structural analysis of spray-dried powders by confocal laser scanning microscopy. *Asia Pac. J. Chem. Eng.* **2**: 41–46.

Teipel, U., 2005. *Energetic materials.* Wiley-VCH, Weinheim, Germany.

Thijssen, H. A. C., Rulkens, W. H., 1968. Retention of aromas in drying food liquids. *De Ingenieur* **80**: 45–56.

Toei, R., Okazaki, M., Furuta, T., 1978. Drying mechanism of a non-supported state, in *Proceedings of 1st International Drying Symposium* (ed. A. S. Mujumdar). Science Press, Princeton, USA, pp. 53–59.

Tuomasjukka, S., Kallio, H., Forssell, P., 2006. Effect of microencapsulation of dietary oil on postprandial lipemia. *J. Food Sci.* **71**: S225–S230.

Ubbink, J., Schoonman, A., 2003. Flavor delivery systems, in *Kirk-Othmer encyclopedia of chemical technology.* John Wiley & Sons, New York.

Uihlein, K., 1993. Butanoxidation an VPO-Wirbelschichtkatalysatoren. Diss., Univ. Karlsruhe, Germany.

van Grieken, R., Markowicz, A. A., 2002. *Handbook of X-ray spectroscopy.* Marcel Dekker, New York, USA.

Vehring, R., 2007. Pharmaceutical particle engineering via spray drying. *Pharm. Res.* **25**: 999–1022.

Velasco, J., Dobarganes, C., Márquez-Ruiz, G., 2003. Variables affecting lipid oxidation in dried microencapsulated oils. *Grasas y Aceites* **54**: 304–314.

Verhey, J. G. P., 1972a. Vacuole formation in spray-dried powder particles, Part 1: Air incorporation and bubble expansion. *Neth. Milk Dairy J.* **26**: 86–202.

Verhey, J. G. P., 1972b. Vacuole formation in spray-dried powder particles, Part 2: Location and prevention of air incorporation. *Neth. Milk Dairy J.* **26**: 203–224.

Verhey, J. G. P., 1973. Vacuole formation in spray-dried powder particles, Part 3: Atomization and droplet drying. *Neth. Milk Dairy J.* **27**: 3–18.

Vrentas, J. S., Vrentas, C. M., 1996. Hysteresis effects for sorption in glassy polymers. *Macromolecules* **29**(12): 4391–4396.

Walton, D. E., Mumford, C. J., 1999a. Spray dried products – Characterization of particle morphology. *Chem. Eng. Res. Des.* **77**(1): 21–28.

Walton, D. E., Mumford, C. J., 1999b. The morphology of spray-dried products: The effect of process variables upon the morphology of spray dried particles. *Chem. Eng. Res. Des.* **77**(5): 442–490.

Walton, D. E., 2000. The morphology of spray-dried particles – a qualitative view. *Drying Technol.* **18**: 1943–1986.

Walz, A., Mayer, M., 1966. Theoretische und experimentelle Untersuchung zur Herstellung von Stein- und Glaswolle. *Glastechn. Berichte* **8**: 359–370.

Walzel, P., 2001. *Proceedings of the 1st Conference on Spray Drying.* TU Dortmund, Shaker Verlag, Aachen, Germany.

Wang, Z. L., Finlay, W. H. *et al.* (2006) Powder formation by atmospheric spray-freeze-drying. *Powder Technol.* **170**: 45–52.

Washburn, W. W., 1921. The dynamics of capillary flow. *Proc. Phys. Rev.* **17**: 273–283.

Wendel, S., Çelik, M., 1997. An overview of spray-drying applications. *Pharm. Technol.* **21**: 124–156.

Whorton, C., Reineccius, G. A., 1995. Evaluation of the mechanisms associated with the release of encapsulated flavor materials from maltodextrin matrices, in

Encapsulation and controlled release of food ingredients (eds S. J. Risch, G. A. Reineccius). American Chemical Society, Washington DC, USA, pp. 143–160.

Williams, G., Watts, D. C., 1970. Non-symmetrical dielectric relaxation behavior arising from a simple empirical decay function. *Trans. Faraday Soc.* **66**: 80–85.

Williams, M. L., Landel, R. F., Ferry, J. D., 1955. The temperature dependence of relaxation mechanisms in amorphous polymers and other glass-forming liquids. *J. Am. Chem. Soc.* **77**: 3701–3707.

Wollny, M., Schubert, H., 1990. Eine neue Methode zur Bestimmung des zeitlichen Benetzungsverhaltens von Partikelschüttungen. *Proceedings of DECHEMA Jahrestagung*, Wiesbaden, Vol. 2, 369.

Wouters, I. M. F., Geldard, D., 1996. Characterizing semi-cohesive powders using angle of repose. *Part. Syst. Charact.* **13**: 254–259.

Yamamoto, S., Sano, Y., 1992. Drying of enzymes: Enzyme retention during drying of a single droplet. *Chem. Eng. Sci.* **47**: 177–183.

Yamamoto, S., Sano, Y., 1994. Drying of carbohydrate and protein solutions. *Drying Technol.* **12**: 1069–1080.

Yaginuma, Y., Ozeki, Y., Kakizawa, M., Gomi, S. I., Watanabe, Y., 2007. Effects of powder flowability on die-fill properties in rotary compression. *J. Drug Delivery Sci. Technol.* **17**: 205–210.

Yoshii, H., Soottitantawat, A., Liu, X.-D., Atarashi, T., Furuta, T., Aishima, S., Ohgawara, M., Linko, P., 2001. Flavor release from spray-dried maltodextrin/gum arabic or soy matrices as a function of storage relative humidity. *Int. Food Sci. Emerg. Technol.* **2**: 55–61.

Yoshii, H., Furuta, T., Fujiwara, M., Linko, P., 2003. Oxidation stability of powdery ethyl eicosapentaenoate included in cyclodextrins and polysaccharide/cyclodextrin mixtures. *Jpn. J. Food Eng.* **4**: 25–30.

Yoshii, H., Ohashi, T., Kugimoto, Y., Furuta, T., Linko, P., 2005. Stability of alcohol dehydrogenase (ADH) during a suspended droplet drying and storage. *Drying Technol.* **23**: 1217–1227.

Yoshii, H., Soottitantawat, A., Iida, K., Ohgawara, M., Furuta, T., 2006. Effect of additives on the formation of hollow particles in spray-dried powder. *Proceedings of 15th International Drying Symposium (IDS2006)*, Budapest, Volume C, 1339–1344.

Yoshii, H., Kawamura, D., Neoh, T.-L., Furuta, T., 2007. *Proceedings of 5th Asia-Pacific Drying Conference*, Hong Kong, 317–322.

Yoshii, H., Buche, F., Takeuchi, N., Terrol, C., Ohgawara, M., Furuta, T., 2008. Effects of protein on retention of ADH enzyme activity encapsulated in trehalose matrices by spray drying. *J. Food Eng.* **87**: 34–39.

Zbicinski, I., Delag, A., Strumillo, C., Adamiec, J., 2002a. Advanced experimental analysis of drying kinetics in spray drying. *Chem. Eng. J.* **86**: 207–216.

Zbicinski, I., Strumillo, C., Delag, A., 2002b. Drying kinetics and particle residence time in spray drying. *Drying Technol.* **20**: 1751–1768.